CUMULATIVE YIELDS IN THE FAST NEUTRON FISSION OF U^{238}

CUMULATIVE YIELDS IN THE FAST NEUTRON FISSION OF U^{238}

By

CHERIAN K. MATHEWS, M.Sc.

A Thesis

Submitted to the Faculty of Graduate Studies

in Partial Fulfilment of the Requirements

for the Degree

Doctor of Philosophy

McMaster University

October 1964

DOCTOR OF PHILOSOPHY (1964)
(Chemistry)

McMASTER UNIVERSITY
Hamilton, Ontario

TITLE: Cumulative Yields in the Fast Neutron Fission of U^{238}

AUTHOR: Cherian K. Mathews, B.Sc. (Kerala University)
M.Sc. (Agra University)

SUPERVISOR: Professor R. H. Tomlinson

NUMBER OF PAGES: viii, 98

SCOPE AND CONTENTS: Isotopic abundances of the elements xenon, cesium, barium, cerium, neodymium, samarium, rubidium and strontium formed in the fast (fission spectrum) neutron fission of U^{238} have been measured using the mass spectrometric method. These ratios were normalized with respect to each other through isobaric nuclides and isotope dilution to obtain the relative yields of isobaric chains in the heavy mass region. By normalizing the heavy mass yields to 100%, the absolute fission yields of twenty-one isobaric chains in the 130 - 154 mass range were determined. The origin of the fine structure in the cumulative yield versus mass curve is discussed. It has been concluded that, while most of the fine structure arises from the variation in neutron emission probabilities, some of it could be the result of the shell effect in the fission process itself.

ACKNOWLEDGEMENTS

The author wishes to express his sincere appreciation for the encouragement and guidance he received from Professor R. H. Tomlinson throughout the course of this work. He also wishes to thank Dr. W. B. Clarke for the help in analysing the rare gas samples.

The author is indebted to the Canadian Commonwealth Scholarship and Fellowship Committee who made it possible for him to come to Canada and to carry out this work.

TABLE OF CONTENTS

LIST OF TABLES

LIST OF ILLUSTRATIONS

I. INTRODUCTION

General Introduction

When a heavy nucleus is bombarded with neutrons it may split into two fragments of medium weight. This phenomenon was first observed by Hahn and Strassmann and given the name fission by Meitner and Frisch. Since the original discovery of the neutron-induced fission of uranium, it has been established that all nuclides in the actinide region can be made to undergo fission by supplying low or moderate excitation energies. In fact, many of these nuclides undergo fission spontaneously, the probability of the process increasing sharply with atomic number; thus the spontaneous fission half-lives range from $> 10^{20}$ years for Th^{232} to about 6 seconds for 102^{254}. It is the short spontaneous fission life-times that limit the synthesis of still heavier elements.

Fission can be induced by bombardment with neutrons, charged particles and gamma rays. Of these, neutron-induced fission is the most widely studied because the neutron, being neutral, can penetrate the nucleus even at low energies. Many heavy nuclides with odd numbers of neutrons, such as U^{235} and Pu^{239}, can be made to fission by bombardment with thermal neutrons, whereas nuclides with even numbers of neutrons, such as Th^{232} and U^{238}, require neutrons having energies above some threshold value. For U^{238} the threshold energy is about 1 Mev and, therefore, if U^{238} is irradiated in a nuclear reactor only a small fraction of the neutron flux is effective in causing fission.

It is fairly well established that fission is a compound nucleus reaction. In the case of neutron-induced fission this means that the neutron enters the target nucleus and the excess energy is dissipated throughout the nucleus to form a 'compound nucleus'. The compound nucleus may then fission into two fragments releasing about 200 Mev of energy in the process. Less frequently other processes, such as gamma emission, particle emission and ternary fission, also take place.

Heavy elements like uranium have a neutron-to-proton ratio in the range of 1.5 to 1.6, whereas the stable nuclides with the masses of the lighter fission products have neutron-to-proton ratios between 1.25 and 1.45. Hence fission fragments are neutron-rich and therefore unstable toward beta decay. The fragments are, however, also highly excited and de-excite themselves through the faster processes of gamma and neutron emission before the slower beta decay begins. The instability of fission products to beta decay leads to decay chains 3 to 4 members in length. A few nuclides formed through beta decay also emit neutrons and hence the delayed neutron emission in fission. The fission process may be imagined to take place in a series of steps as illustrated in Fig. I-1. The fact that 2 to 3 neutrons are emitted per fission made it possible to have chain reaction in fissile materials and this, coupled with the large energy release per fission, led to nuclear bombs and power reactors.

There are a very large number of ways in which a heavy nucleus can undergo fission to form two fragments. The probabilities of the various modes of fission are expressed in terms of fission yields. The prompt yield of a fission fragment is the percentage of fissions which give rise to that fragment before neutron emission. The independent

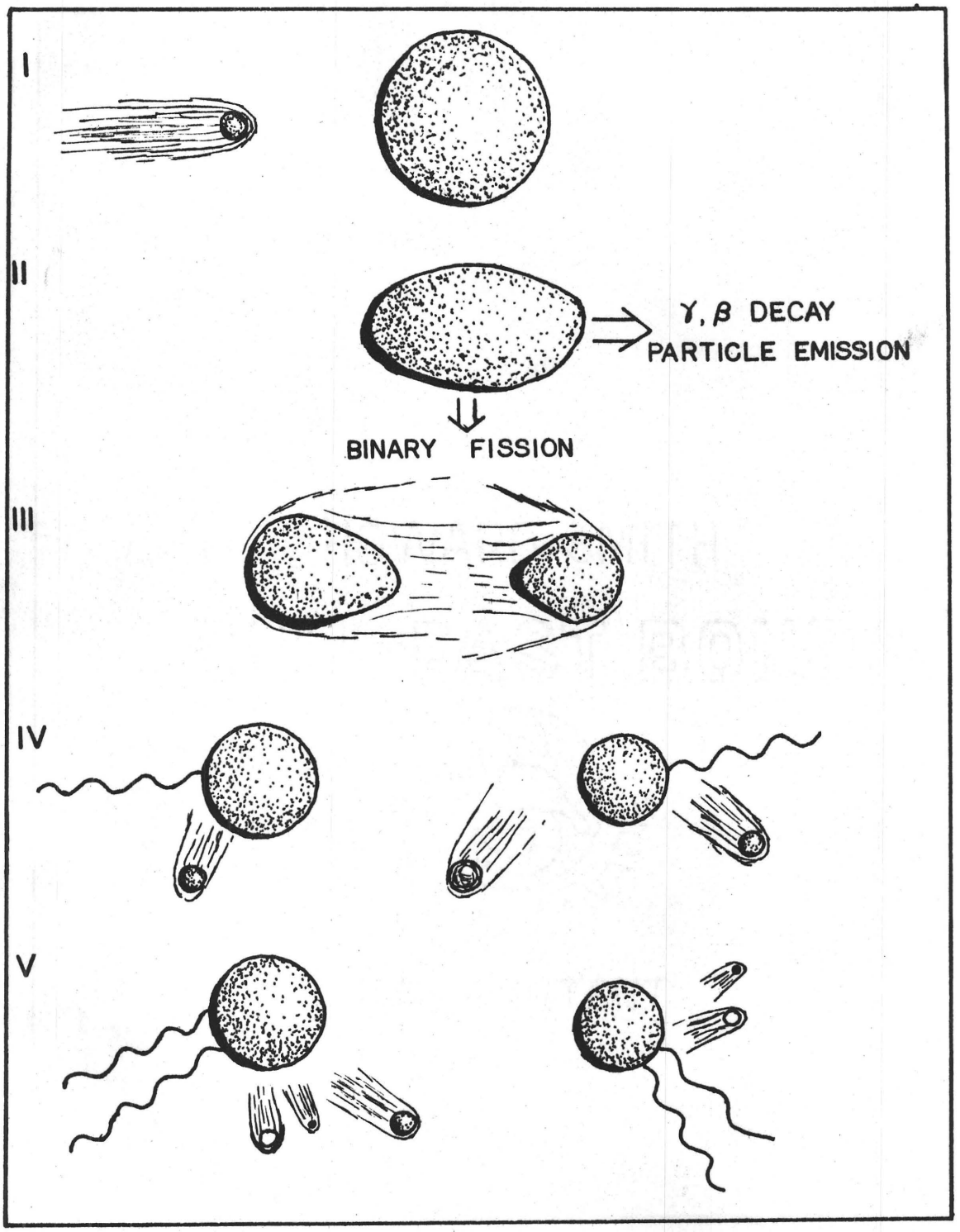

FIG. I-1: A Schematic Representation of the Fission Process

I. Neutron bombardment of a heavy nucleus
II. The compound nucleus
III. Prompt fission fragments
IV. Emission of prompt neutrons and gamma rays from fragments
V. Beta decay, delayed-neutron emission

yield of a fission product nuclide is the percentage of fissions which result in the formation of that particular nuclide before any beta decay takes place. Here we distinguish between fission fragment and fission product; the former is produced at the instant of fission and the latter is formed either independently or through decay of fission fragments. The sum of the isobaric independent yields is known as the cumulative chain yield. Since earlier members of a chain decay to form later members, thus ending up in a stable nuclide, one can measure the cumulative yield of the chain by simply measuring the yield of the last member of the chain after allowing sufficient time for the complete decay of the earlier members. Quite often it is possible to obtain the cumulative yield of a chain from the yield of a member one or two charge units removed from stability by correcting for decay and the independent yields of the succeeding members.

The low energy fission of heavy elements is predominantly asymmetric. When the yields are plotted against mass numbers of fission products a double humped curve is obtained which has a minimum at the mass value corresponding to symmetric fission. The balance between symmetric and asymmetric fission depends on the excitation energy of the compound nucleus as well as on the nature of the fissioning nucleus. This is usually expressed in terms of a peak-to-trough ratio, defined as the ratio of the fission yields corresponding to the two maxima in the mass distribution and the yield at the minimum. The peak-to-trough ratio is greatest for spontaneous fission, next greatest for fission with neutrons of selected resonance energy, slightly lower for slow neutron fission and markedly lower for fast neutron fission. As the bombarding energy is increased, the ratio becomes lower until in high energy fission symmetric splitting predominates.

The sum of all yields in the binary fission of a given nucleus should add up to 200% and this fact has been used in normalizing relative yield data. Since the peak-to-trough ratio is more than 100 for low energy fission, the mass-yield curve is essentially made up of the two peaks corresponding to the light and heavy fragments and each of these can be normalized to 100% without appreciable error.

The determination of accurate fission yields is of considerable importance, not only in nuclear technology but also in nuclear theory; for an adequate theory must account for all the features of nuclear fission. Such a theory is yet to be found; but it must be hoped that more detailed information would point the way.

Radiochemical techniques which led to the discovery of fission were also successfully used in studying fission yields. In this method a known amount of a non-radioactive carrier of a given fission product is added to the solution of irradiated fissile material. After ensuring complete exchange between the carrier and the fission product, the solution is subjected to an analytical procedure designed to separate the element of interest from the solution in a state of chemical and radioactive purity. From a measurement of the radioactivity and the chemical yield of the separated sample, it is possible to calculate the number of atoms of the fission product in the original solution. In determining relative fission yields it is only necessary to compare the radioactivities of the separated elements. The radiochemical method suffers from errors arising out of counting techniques, incomplete knowledge of decay schemes, etc., which have limited the reliability of most of the published yields to at least 10%.

The introduction of the mass spectrometric method in the study of fission yields was a great improvement because isotopic abundance ratios could be determined to better than 1% accuracy. In the actual method used, the isotopic abundances for the various elements produced in fission are measured in the mass spectrometer and they are related to each other either by isotope dilution or through isobars. The absolute yields obtained this way are accurate to better than 5% in most cases. Also, stable end products could be analysed in the mass spectrometer, which has made it practical to obtain yields at almost every mass. It was the use of mass spectrometric techniques that led to the discovery of fine structure in mass-yield curves of fission products. The mass spectrometer does, however, require relatively large sample sizes and for short-lived fission products the radiochemical method is more sensitive.

Mass spectrometric techniques have been applied so far only to nuclides such as U^{235}, U^{233}, Pu^{239} and Pu^{241}, which have high thermal cross sections. From these nuclides sufficient quantities of fission products can be produced with a rather short irradiation in a nuclear reactor. However, nuclides such as Th^{232} and U^{238} have not been previously studied because of the difficulty in analysing the very small quantities ($< 10^{-9}$ g) of fission products that are produced in normal reactor irradiations. Not only is the fission rate low by virtue of the relatively small cross sections and available neutron fluxes above threshold, but long irradiations do not solve the problem of obtaining samples which are reasonably large. On irradiation, U^{238} nuclei capture neutrons to form U^{239} which decays through Np^{239} to Pu^{239}. Pu^{239} has a large fission cross section and hence, in long irradiations of U^{238}, fission of Pu^{239} makes a significant contribution to the total number of fissions. The

difficulty in analysing small samples arises not only from the point of view of the sensitivity of the mass spectrometer but also because of the possibility of contamination. Natural contamination in fission product samples interferes with the abundance measurements. In the case of some elements, it is possible to correct for small amounts of contamination; but in other cases minimizing contamination to negligible amounts is the only way to getting accurate measurements. It is difficult, however, to keep small samples free of contamination during the chemical processing and analysis.

The present work reports the measurement of the fission yields in the fast neutron fission of U^{238} by mass spectrometric techniques. By fast neutrons we mean the fission spectrum neutrons above the fission threshold. This is the first time such small fission product samples have been analysed in the mass spectrometer. A study of the isotopic abundance ratios of elements xenon, cesium, barium, cerium, neodymium and samarium has made possible the determination of the fission product yields from masses 131 to 154 with an accuracy of about 3%. The fission product samples obtainable were not large enough to make a similar complete study of the light mass region. The fine structure and other features of the mass distribution are discussed.

Historical Background

In the latter half of the 1930's several scientists were working on the identification of the activities produced in the neutron irradiation of uranium. Through a series of careful experiments, Hahn and Strassmann (39H1, 39H2) were able to establish that one of the activities

produced was an isotope of barium. Meitner and Frisch (39M1) correctly interpreted the result as due to the fission of uranium into two fragments of medium weight. These authors also recognised that an exceptionally large amount of energy should be liberated in the reaction. This was soon verified by Frisch (39F1), making use of the ionizing property of fission fragments. From a study of the ion chamber pulses, Jentschke and Prankl (39J1) concluded that there were two groups of fission fragments -- one centered at an energy of about 60 Mev and the other centered at about 100 Mev. This was the first evidence for asymmetry in fission. The same year, von Halban, Joliot and Kowarski (39vonH1) detected the emission of neutrons produced in the fission process.

Most of the early study of fission yields has been made using the techniques of radiochemistry. This method was much superior to the physical methods then available. Early workers in the field included Hahn and Strassmann (39H3), Moussa and Goldstein (41M1) and Anderson, Fermi and Grosse (41A1). Extensive investigations of the fission yields in the low energy neutron-induced fission of U^{233}, U^{235}, U^{238} and Pu^{239} were made by a large group of American scientists during 1942-48 under the Manhattan Project. This work was classified at that time, but has since been published by Coryell and Sugarman (51C1). Similar Canadian studies were reported by Grummitt and Wilkinson (48G1). Since the end of the war, radiochemical data have been substantially improved, both in quantity and in quality. All these results confirmed the asymmetric nature of low energy fission; the mass distribution was double-humped. In the case of U^{235}, the mass-yield curve showed maxima at about 140 and 95 mass units. It was also observed that on increasing the mass of the

fissioning nucleus the heavy mass peak remained in about the same position, whereas the light mass peak moved towards higher mass region. Considering the errors involved in the radiochemical method, a smooth curve was always drawn through the data points and, hence, radiochemical measurements did not indicate any fine structure in the mass distribution.

Thode and co-workers (47Th1, 50M1) introduced mass spectrometric techniques in the study of fission. These authors measured the abundance ratios of the isotopes of the rare gases produced in fission and established the existence of fine structure in fission yield curves. This was soon confirmed by other workers (49G1, 51G1, 53P1). In the following years, solid source mass spectrometry and isotope dilution techniques were successfully used in the study of fission yields by Steinberg and Glendenin at Argonne (56S1) and by Tomlinson and co-workers at McMaster University (55P1, 59B1, 59F1, 62F1). The latter group has published accurate mass spectrometric measurements of fission yields in the slow neutron fission of U^{233}, U^{235}, Pu^{239} and Pu^{241}.

Meanwhile, physical methods were developed to a degree of accuracy comparable to radiochemical method. Improved ionization chamber techniques have resulted in the accurate measurement of kinetic energy distributions of fission fragments (50Br1, 50Br2). Prompt fission yields were measured, using the time-of-flight method, by several authors, notably Leachman and co-workers (52L1, 54L1), Stein (57S1) and Milton and Fraser (58M1, 62M1). The latter authors were also able to measure neutron emission probabilities from different fission fragments. Neutron emission as a function of fragment mass can also be obtained by combining prompt yield data obtained from time-of-flight studies and cumulative

yield data from radiochemical and mass spectrometric studies. This information was deduced for a number of fissioning nuclides by Terrel (62T1). All these studies were made on a few fissile nuclides -- mainly U^{233}, U^{235}, Pu^{239} and Cf^{252}. It is necessary to obtain accurate fission yields -- prompt, independent and cumulative -- in the fission of other heavy nuclides in an effort to arrive at a better understanding of the fission process.

Fission of U^{238}

The first reported study of the fission yields from U^{238} was made by Engelkemeir et al (51E1). These authors irradiated depleted uranium in cadmium-lined capsules in a nuclear reactor and measured the yields of twelve nuclides using radiochemical techniques. The mass distribution curve had the usual double-humped nature. A more detailed investigation using improved techniques was carried out by Keller et al (54K1). They measured the yields of fifteen fission product nuclides and essentially confirmed the results of Engelkemeir and others. The peak-to-trough ratio obtained by Keller et al was, however, about 200, which was several times the value reported by the earlier workers.

In 1955 Wanless and Thode (55W1) measured the relative yields of the isotopes of krypton and xenon in the fast (fission spectrum) neutron fission of U^{238}. This mass spectrometric measurement showed the existence of fine structure in both the regions studied. Katcoff (60K1) combined all the results quoted above and plotted a smooth mass-yield curve which did not show any fine structure, except those arising from the mass spectrometric results for rare gases. All the published results on the mass distribution in the fast fission of U^{238} are given in Tables I-1 and I-2.

TABLE I-1

Radiochemical Yields of the Heavy Mass Fission Products in the Fast Fission of U^{238}*

Mass No.	Yield
127	0.13 ± 0.03
132	4.7 ± 0.7
137	7.1 ± 0.7
140	5.7[a]
144	4.9 ± 0.5
156	0.073 ± 0.01

*Taken from ref. (54K1).

[a]Used as reference yield.

TABLE I-2

Fast Fission of U^{238}
Heavy Mass Yields Listed by Katcoff[*]

Mass No.	Yield
127	0.12
131	3.2[a]
132	4.7[a]
133	5.5[b]
134	6.6[a]
135	6.0[b]
136	5.9[a]
137	6.2
140	5.7
144	4.5
147	2.6
149	1.8
153	0.41
156	0.071
159	0.0084
161	0.0016

[*]Ref. (60K1).

[a]Mass spectrometric data from Wanless and Thode (55W1).

[b]Tentative mass spectrometric data communicated by R. H. Tomlinson, McMaster University (60T1).

Several authors have measured the yields in the fission of U^{238} by 14 Mev neutrons using radiochemical methods (58Pr1, 58C1, 58Fd1). All of them report mass distributions with two maxima and a peak-to-trough ratio of 5 to 10.

It is clear that a more detailed study is called for to investigate the fine structure and other features of U^{238} fission.

II. THE THEORY OF NUCLEAR FISSION

Mathematically the complete description of a nucleus is contained in its total wave function. Starting from this, one should, in principle, be able to explain all nuclear reactions, including fission. But our present state of knowledge is far from such a complete description of the nucleus; not only do we lack a clear understanding of internuclear forces but also we cannot solve many-body problems exactly. Hence we resort to models which attempt to reproduce the essential characteristics of the actual system.

The Liquid Drop Model

Bohr and Wheeler (39B1) made use of the liquid drop model to explain fission. Here the fissioning nucleus is treated as a uniformly charged incompressible drop of liquid. The actual Hamiltonian of the nucleus is replaced with the simple classical approximate Hamiltonian of the charged liquid drop.

The forces operating among the nucleons in a nucleus are the short-range, charge-independent, nuclear forces and the Coulomb repulsion forces of the protons. The total energy of the nucleus can be expressed as the sum of a volume term, a surface correction and the Coulomb energy. The shape assumed by the nucleus is dependent on the surface tension and the Coulomb forces.

For a stable nucleus, the sum of the surface and Coulomb energy changes must be positive for any small distortion from equilibrium. But for certain types of distortions of the charged drop (such as the stretch

to give axially symmetric shapes) the Coulomb term overtakes the surface term if the distortion is increased beyond a certain point. Eventually the drop may divide into two or more fragments. Only the very heaviest elements have sufficiently high nuclear charge that relatively small deformations can lead to fission.

Expanding the radius of a distorted sphere in terms of Legendre Polynomials,

$$R(\theta) = R\,(1 + \alpha_0 + \alpha_2 P_2(\cos\theta) \ldots\ldots)$$

Bohr and Wheeler were able to estimate the distortion energy in terms of the surface tension '0' and the nuclear charge (Z):

$$\Delta E = 4\pi R^2 0 \left[\frac{2}{5}\alpha_2^2 + (\text{higher powers of } \alpha_2)\right] - \frac{3}{5}\frac{(Ze)^2}{R}\left[\frac{1}{5}\alpha_2^2 \ldots\ldots\right]$$

Examination of the coefficients of α_2^2, viz,

$$4\pi R^2 0\ \frac{2}{5}\left[1 - \frac{3}{10}\frac{(Ze)^2}{R}\cdot\frac{1}{4\pi R^2 0}\right].$$

makes it clear that with increasing value of the ratio Z^2/R^3 we come finally to the limiting value,

$$Z^2/R^3 = \frac{4\pi 0}{e^2}\left(\frac{10}{3}\right)$$

or
$$Z^2/A = \left(\frac{10}{3}\right)(4\pi R_0{}^3 0/e^2) \qquad (\text{Since } R = R_0 A^{1/3})$$

beyond which the nucleus is no longer stable with respect to the deformations of the simplest type. The actual value of $(Z^2/A)_{\text{limiting}}$ can be calculated with the help of the semi-empirical mass formulas. Using recent constants (54G1) we find,

$$(Z^2/A)_{\text{limiting}} = 50.13.$$

Bohr and Wheeler defined the fissionability parameter 'x' of a nucleus as the ratio of its (Z^2/A) to $(Z^2/A)_{limiting}$. When x is close to one, small distortions would lead to fission. When $x \ll 1$, the nucleus is stable to distortions of the $P_2(\cos\theta)$ type.

It is clear that some minimum energy must be supplied to the liquid drop to bring it to the critical shape from which it can fly apart on its own. This critical energy for fission can be calculated if the critical shape is known. The accuracy of the calculated critical energy depends on the closeness to which the critical shape is approximated. Even for a simple uniformly charged incompressible liquid drop this is a formidable problem. In order to describe an arbitrary distortion one needs an infinite number of parameters and, in principle, the problem is that of locating those distortions which have 'extremum' values with respect to all these parameters. In practice, one tries to guess plausible shapes for the critical deformations and to choose coordinates that represent these in the simplest possible way. If one finds a saddle point by doing this limited type of problem, it seems, however, that there is no simple way to know how close it is in shape or in energy to the true saddle point of the liquid drop. Bohr and Wheeler found the saddle point shape for the α_2 and α_4 type of deformation and expressed the deformation energy as a function of x. Many later workers, notably Swiatecki and co-workers, have given more exact calculations for the critical energy. The agreement with observed values is not very good, as seen from Table II-1.

The difficulty in finding the saddle point shape is only one of the problems in the application of the liquid drop model to fission. The distortion energy at the saddle point comes in as the difference

TABLE II-1*

Comparison of Observed Thresholds with Liquid Drop Calculations

Nuclide	Z^2/A	x	$E_{thres.}$ (Mev)	$E_{obs.}$ (Mev)
Th^{232}	34.914	0.6969	15.08	5.95
Th^{233}	34.764	0.6939	15.58	6.44
Pa^{232}	35.694	0.7125	12.68	6.18
U^{233}	36.326	0.7251	10.96	5.49
U^{235}	36.017	0.7189	11.79	5.75
U^{237}	35.713	0.7129	12.63	6.40
U^{238}	35.563	0.7099	13.06	5.80
U^{239}	35.414	0.7069	13.51	6.15
Np^{237}	36.494	0.7285	10.53	5.49
Np^{238}	36.340	0.7254	10.92	6.04
Pu^{239}	36.971	0.7380	9.39	5.48

*Taken from (62H1).

between two rather large energies. A small error in either of these energies can bring about great changes in the estimated threshold energy. Moreover, 'small' energies that are normally overlooked may actually be relatively important as regards fission. Such normally neglected energies include those associated with nuclear compressibility, the uneven distribution of charge in the nuclear volume and the polarizability of the charge distribution. One may expect non-classical effects associated with individual nuclear levels that must be considered at about 6 Mev excitation.

One of the biggest failures of the liquid drop model is that it is not capable of explaining asymmetric fission. The original paper of Bohr and Wheeler suggested that as the fissionability parameter decreased below 1, the critical shape started developing a concavity around the equatorial belt and hence symmetric fission was favoured for nuclides with x significantly different from 1. Recent investigations by Swiatecki and Cohen have shown, however, that in the case of x values above 0.7 the saddle point shape does not at all suggest two separating fragments; hence one cannot predict, without a calculation of the dynamic effects, what might happen between the saddle and scission points. Thus it is not correct to say that the liquid drop model predicts symmetric fission; but it does not explain the asymmetry in the mass distribution.

Cohen and Swiatecki (62C1) point out that a complete theory of fission based on the liquid drop model will consist of the following steps. First, the potential energy and kinetic energy of the deformed charged drop must be calculated to establish the complete Hamiltonian. Then the equations of motion of the system for different initial conditions must be solved. The large number of possible initial conditions

will call for a discussion of the Statistical Mechanics of the problem in order to correlate average initial conditions with average end results of the division. On completion of the classical solution, the next step will be to replace the conjugate momenta in the Hamiltonian with quantum mechanical operators and to study in an analogous way the quantum-mechanical and quantum-statistical properties of the resulting Schrödinger equation.

At the present time we are far from a theory of fission of an idealized liquid drop, and even further from the theory of the fission of a nucleus, since a nucleus is at least as complicated as an idealized drop.

Fong's Statistical Theory of Fission

In 1953, Fong proposed a statistical theory of fission (53F1). He pointed out that the fission process is sufficiently slow for a nucleon to cross the nucleus many times as the nucleus moves from the saddle point to scission and, therefore, an instantaneous statistical equilibrium is established at any instant of the process. It follows then that the relative probabilities of various fission modes are proportional to the densities of the quantum states of the corresponding nuclear configurations at the moment when statistical equilibrium is last established, presumably the moment just before separation.

Fong approximated the nuclear configuration at this critical moment by two deformed fragments in contact. For simplicity it was further assumed that the deformation was of the $P_3(\cos\theta)$ type (where P_3 is the third Legendre Polynomial) and that, at the moment just before separation, the two deformed nuclei are in contact at their tips and oriented such that their axes coincide. The P_3 term is chosen because the corresponding

deformed shape roughly approximates the egg-shaped fragment resulting from the scission of a dumb-bell-shaped parent nucleus. Using this approximation, Fong was able to calculate the potential energy of the system as the sum of the Coulomb energy and the deformation energy.

In order to calculate the total energy release, Fong derived his own semi-empirical equation for the masses of the primary fission fragments, making allowance for shell-effects in the mass surface. The difference between this total energy release and the potential energy of the system at scission gives the energy available for internal excitation and the energy of the centre-of-gravity motion (k) of the fragments at the critical moment. The density of excitation states of a fragment was taken from the general statistical model of the nucleus to be

$$W_o(E) = C\, e^{2\sqrt{a\,E}}$$

where a and C are empirical parameters evaluated from other data and E is the excitation energy.

The probability of a given mode of fission is then proportional to the product of the density of states of the fragments in contact and the density of momentum states corresponding to translational motion. The density of quantum states depends on the mass numbers, charge numbers and deformation shapes of the fission fragments. By finding the deformation shape corresponding to the minimum potential energy, the author was able to obtain the relative probability of the fission mode specified by given mass and charge numbers. By integrating over the charge numbers the relative probability for a given mass ratio is obtained.

Using this method, Fong was able to obtain a mass distribution curve for U^{235} which agreed well with experimental data. Perring and Storey (55P2) applied this theory in the case of Pu^{239} and found little agreement between the calculated and the experimental mass distributions; however, Fong was able to get better agreement with experimental data using a revised choice of parameters in his mass equations.

Another failure of Fong's theory is its inability to reproduce the experimentally observed distribution of the total kinetic energy as a function of mass ratio of fragments. The kinetic energy distribution obtained by Fong in his original work was maximum for symmetric fission and fell off as the asymmetry increased. Recently, the author corrected this error (63F1) by assuming $P_2(\cos\theta)$ type of deformation in place of the earlier $P_3(\cos\theta)$ type. After Bohr, Mottelson and co-workers (56A1), the radius of the deformed nucleus was represented by $R(\theta) = R\left[1 + \beta P_2(\cos\theta)\right]$ where β is a deformation parameter. The deformation energy is then $\frac{1}{2} C_2\beta^2$ where C_2 is a constant for a given nucleus. Using the experimental C_2 values given by Mottelson and co-workers, Fong obtained C_2 as a function of mass number and calculated the deformation energies of the fragments. By this method the author was able to calculate a kinetic energy distribution which agreed reasonably well with experimental data. The new approach, however, does not even predict asymmetric fission and the author attributes this to the fact that the deformation energy calculated is very inaccurate in the region of symmetric fission.

Even though the predictions from Fong's theory do not agree well with experimental observations, the author maintains that this is due to the deficiency of the physical data used in the theory rather than the basic

assumption itself. A detailed application of the statistical theory requires information on nuclear masses, on nuclear level density and on nuclear deformability. The fact that the mass distribution and prompt neutron yield curves of all fissioning nuclides coincide in the heavy fragment region tends to support the argument that the fission process is determined by the fission products rather than by the fissioning nuclides. This evidence strongly suggests that factors at some time late in the fission process play a dominant role.

Fission as a Barrier Penetration Process

Another approach to fission which focusses attention at the moment of scission is the barrier penetration model. Frenkel (46F1) was the first to look for an explanation of the asymmetric mass distribution in the barrier penetration probabilities of different configurations at the point of scission. Recalling the Bohr and Wheeler expression for the probability of barrier penetration in spontaneous fission,

$$\exp\left[\left(\frac{-2^{3/2}}{\hbar}\right)\int\left\{\left(\begin{array}{c}\text{potential energy}\\ \text{minus available energy}\end{array}\right) \times \left(\begin{array}{c}\text{effective}\\ \text{mass}\end{array}\right)\right\}^{1/2} d(\text{distance})\right]$$

he ascribed the greater probability for unequal division to the smaller value in this case of the reduced mass of the system. However, Hill and Wheeler (53H1) have pointed out that if the difference in the reduced mass of the system were to account for the observed difference in probabilities between symmetric and asymmetric fission, the absolute probability of fission would be so low that fission would virtually be non-observable.

In 1961 Brunner and Paul (61B1) put forward a barrier penetration model in which the probability of a given mode of fission depended on the deformation of the fragments at the moment of separation. The deformability of the fragments is strongly influenced by shell structure; the

minimum deformation occurs when the neutron or proton number of one of the fragments is magic. This leads to two magic effects: (1) The nuclear force potential between two fragments is, for a fixed value of the distance between their centres, higher (i.e., lower in absolute value) when one of the fragments is a magic-number-nucleus. (2) The distribution of the mean total kinetic energy exhibits maxima for the same mass ratios. The combination of these two effects makes the barrier height above the tunnelling point a function of the mass ratio of the fragments; the probability of tunnelling is highest for asymmetric fission.

The deformation of the fragments is calculated as follows. The total energy of the system is given by the mass of the compound nucleus. At the moment of scission this is made up of the masses of the fragments, their deformation energy, and the Coulomb energy of repulsion between them. After the fission event, the total energy becomes the sum of the masses of the fragments, their excitation energy and their kinetic energy.

$$M^{*}c^{2} = (M_1 + M_2)c^2 + E_1 + E_2 + T$$

Here M^{*} is the mass of the compound nucleus including the excitation energy, M_1 and M_2 are the masses of the primary fragments, E_1 and E_2 their excitation energies and T the total kinetic energy of the fragments. Brunner and Paul assumed that for a given mode of mass division the total charge of the fissioning nucleus is split in the ratio of the fragment masses. Using Fong's mass formula for primary fragments, they calculated $(M_1 + M_2)c^2$ and, subtracting this and the experimental kinetic energy from the total energy, they were able to calculate $E = E_1 + E_2$ for a given mass division. By further assuming that the excitation energy E was

shared between the fragments in the ratio of their masses they obtained E_1 and E_2. The excitation energy E_i was then identified with the deformation energy of the fragment at the moment of scission. The authors assumed, after Bohr and Wheeler, that the deformation was of the $P_2(\cos\theta)$ type, but also considered surface tension (σ) as a function of the mass of the fragment. Thus the deformation energy is given by

$$D_i = \frac{3}{25} \times \frac{e^2}{R_o} \left(\varepsilon \frac{\sigma_i}{\sigma_o} A_i^{2/3} - Z_i A_i^{-1/3} \right) \alpha_i^2$$

where the subscript i represents a given fragment, ε is $(Z^2/A)_{\text{limiting}}$, σ_o is the value of surface tension in the simple liquid drop model, and the other symbols have their usual meaning. Knowing D_i, the deformation parameter α_i is determined.

The variation of σ_i/σ_o with neutron number was obtained from the C_2 values discussed above (56Al). The deformation of the fragments, regarded as a function of the mass ratio m, is thus essentially determined by two factors; firstly, the variation of E with m and, secondly, the variation of σ with m. The second effect is more important; it causes pronounced minima in the curve of α against the neutron number N if a fragment has the magic neutron number N = 50 or N = 82. In other words, the fragments with magic neutron numbers have smaller deformation than others.

If the fragments are in contact with their $\theta = 0$ axes collinear, then the distance between the centres is given by

$$s_o(m) = \left[1 + \alpha_1(m)\right] R_1 + \left[1 + \alpha_2(m)\right] R_2$$

where R_i is the radius of an undeformed spherical fragment.

The authors assumed a nuclear force potential between the fragments of the form

$$V_k(m,s) = - \hat{V}_k e^{-\mu \left[s - s_o(m) \right]}$$

where $\mu = \frac{m_\pi c}{\hbar}$, m_π being the mass of π mesons, $-\hat{V}_k$ is the nuclear potential corresponding to two spherical fragments in contact, and s is the distance between the centres of the fragments. It is further assumed that $\hat{V}_k$ is independent of m. Brunner and Paul showed that for U^{235}, $\hat{V}_k \approx 135$ Mev.

The total potential energy of the system of two fragments is the sum of the Coulomb energy and the nuclear potential.

$$V_{(s)} = \frac{Z_1 Z_2 e^2}{s} - \hat{V}_k \exp \left[- \mu \, (s - s_o) \right]$$

The relative fission probability w is then given, in the WKB approximation, by

$$w = \exp \left[- \frac{2\sqrt{2\nu}}{\hbar} \int_{s_1}^{s_2} \sqrt{V(s) - T} \; ds \right]$$

where ν is the reduced mass of the two-particle system, s_1 and s_2 are the classical turning points of motion, and T is the energy of the virtual state which later appears as the total kinetic energy for the particular mass division. The absolute value of V_k is minimum for a given s when one of the fragments is a magic-number-nucleus, whereas T(m) is maximum for the same situation. The net effect is to give w its maximum value at an m value slightly higher than that corresponding to the magic neutron number of 82 in fragments. For U^{235} the maximum fission probability appears at m = 1.45.

The authors thus obtained qualitative agreement with experimental mass distribution in the fission of U^{235} and Cf^{252}. They pointed out that quantitative agreement cannot be expected on account of the approximations made. These approximations include the use of Fong's mass formula for primary fragments, the arbitrariness in choosing the variation of surface tension with fragment mass, and the restriction to the quadratic term in the expression for deformation energy.

Some of the assumptions made by Brunner and Paul are open to criticism. They ignore charge distribution in fission and assume that the total charge of the fissioning nucleus is split in the ratio of the fragment masses. The apportioning of the total excitation energy in proportion to the masses of the fragments has no experimental foundation. The assumption that the various scission configurations are formed with equal probability is also open to question. In addition, the theory demands the prior knowledge of the kinetic energy distribution of the fragments.

The Unified Model and Fission Theory

Bohr (56B1) has discussed the effect of the quantum states of the compound nucleus in fission. At the saddle point the compound nucleus is 'cold', since most of its excitation energy is tied up as potential energy of deformation. Only a few widely spaced levels are available as fission channels and the spins and parities of these levels will probably play a dominant role in the fission process. Asymmetry in fission is probably related to the existence of low-lying 1^- levels. At higher energies, many fission channels become available and asymmetry effects are less significant.

None of these models can quantitatively describe the fission process, particularly the mass distribution with which we are concerned. The liquid drop model lacks the mathematical simplicity expected in a model. It does not yield its implications readily, nor is it easy to know what modifications are required to make it an effective description of fission (Halpern, 59H1). The other models are very sensitive to data such as mass formulas, surface tension and level densities, which are not accurately known. Hence, it is difficult to test if the fundamental assumptions involved are correct. The implication of all these is, perhaps, that fission is a very complicated process.

III. EXPERIMENTAL

In the experimental procedure used, samples of depleted uranium were purified and irradiated in the reactor. Fission products were extracted from the irradiated samples and the isotopic composition of the elements of interest was measured in a mass spectrometer.

All chemical reagents used were specially purified to remove traces of natural contamination. Distilled water was deionized by passing it through a cation exchange column and this 'ion-free' water distilled in quartz to get the 'pure water' used in all chemical operations. Nitric acid was distilled four times in a quartz still, diluted to 6N, and stored in polythene bottles for use. The 'pure hydrogen peroxide' used was obtained by distilling C.P. hydrogen peroxide under reduced pressure. The glass and polythene ware used in the separation procedures were cleaned by rinsing several times with purified nitric acid and water.

Sample Preparation

The samples irradiated consisted of depleted uranium as U_3O_8. The uranium was first treated to remove any natural contamination. The elements of interest (alkali metals, alkaline earths and rare earths) were produced by fission only in amounts of the order of 10^{-9} g or less. Hence, it was necessary to keep contamination from the naturally-occurring isotopes of these elements to a couple of orders of magnitude less than this to achieve good accuracy in the measurements of the relative isotopic

abundances in fission. Preliminary experiments using typical radioactive tracers showed that a single precipitation with hydrogen peroxide followed by washing gave a decontamination factor of about 70 for rare earths, while the separation was better for alkali and alkaline earth metals.

The following procedure was used to purify the samples. Depleted uranium was dissolved in nitric acid and the solution was evaporated to dryness. The residue was repeatedly taken up in 'pure water' and evaporated to dryness to make the final solution nearly neutral. The solution thus obtained was chilled and uranium peroxide was precipitated using hydrogen peroxide. The precipitate was centrifuged and washed with purified water. This procedure was repeated three to four times to get pure uranium. The purified uranium peroxide was then ignited in a platinum crucible and samples of U_3O_8, weighing about one gram each, were sealed in quartz capsules for irradiation.

Irradiations

The irradiations were carried out in the core of the McMaster University swimming pool reactor. The samples, sealed in quartz capsules, were wrapped in cadmium (about 0.030" in thickness) to cut off thermal neutrons, thus minimizing contributions from the fission of U^{235} and Pu^{239}.

Since it was important to produce as much fission products as possible, it was desirable to use the maximum possible irradiation time. In the case of short-lived nuclides, the irradiation time was limited by the half-life. Even in the case of long-lived and stable fission products, indefinite irradiation was not possible because, in very long irradiations, the contribution from the fission of Pu^{239}, produced by neutron capture in U^{238}, became significant.

A detailed investigation of the contribution of plutonium fission showed that, for irradiations of about 50 days duration, fission of Pu^{239} contributed less than 3% to the total number of fissions (see Appendix A). Since in the region of interest the yields in Pu^{239} fission are not expected to differ appreciably from the yields in U^{238} fission, the error introduced by plutonium fission is negligible for irradiation times of about 50 days or less.

Thus the irradiation times used varied from 5 to 55 days, depending upon the element studied. Table III-1 gives the irradiation data for the various samples.

Extraction of Fission Products

After suitable cooling periods, the fission products were extracted from the irradiated samples. First the capsule was broken and the sample transferred to a centrifuge tube. This procedure did not involve the significant loss of fission products as (1) the fraction lost through recoil from one gram of U_3O_8 contained in a small capsule was negligible and (2) the loss of gaseous fission products through diffusion in U_3O_8 was found to be insignificant by Clarke (62C1).

The sample was dissolved in pure nitric acid and evaporated to dryness. The residue was taken up in water and, by repeatedly evaporating to dryness and dissolving in water, an almost neutral solution was obtained. Peroxide precipitation in the cold removed the bulk of uranium. This procedure was repeated to ensure that no visible solid was left on evaporating the sample to dryness.

The fission product solution thus obtained was evaporated to a small drop on a piece of teflon and transferred to the sample filament of the mass spectrometer. This, when evaporated to dryness under an

TABLE III-1

Irradiation Data

Sample	Irradiation Time (Days)	Cooling Time[a] (Days)	Thermal Flux[b]
A	15.0	5.6	1.5×10^{13}
B	30.0	45.0	1.5×10^{13}
C	53.9	186	1.4×10^{13}
C'	53.9	788	1.4×10^{13}
D	53.9	345	1.4×10^{13}
D'	53.9	840	1.4×10^{13}
E	5.0	5.04	1.0×10^{13}
F	5.0	8.72	1.0×10^{13}
G	50.0	165	7.0×10^{12}
H	50.0	229	7.0×10^{12}
I	50.0	230	1.0×10^{12}
J	10.0	0.21	5.7×10^{12}
K	29.3	41	5.7×10^{12}
L	10.3	3.3	5.7×10^{12}
M	30.26	9.2	5.7×10^{12}

[a]This is the cooling time up to the point where chemical separation was started. In most cases, decay corrections had to be made to the time of measurement.

[b]Cadmium ratio for cobalt is approximately 15.

infra-red lamp, provided an almost invisible coating on the filament. Visible amounts of solid matter seriously affected the ionization efficiency of the source.

Mass Spectrometry

The isotope ratios of the various elements studied in this work (except xenon) were measured using a 25-cm radius, 90° sector, solid-source mass spectrometer of conventional first order direction focussing type as described by D. E. Irish (56I1). It used an accelerating potential of about 3000 V and featured magnetic scanning. With object and collector slits at 0.15 mm and 0.5 mm, the machine had a theoretical resolving power of 385.

a. Ion Production

A multiple filament surface ionization source was used to produce ions of fission products. This source was essentially the same as the one described by Inghram and Chupka (53Inl) with the beam centring plate omitted. It incorporated an ionizing filament in the centre and two sample filaments on either side, with provision for passing suitable currents through them for heating purposes. The filaments were made of tungsten ribbon, 0.001" thick and 0.030" wide. The sample, which was loaded as an essentially weightless film, could be evaporated off the sample filament at a convenient temperature and ionized at the hotter ion filament. Further, since both evaporation and ionization are highly temperature dependent, one could arrive at suitable filament temperature combinations for each element to the exclusion of all others.

Each time a new sample was analysed, the filament holder assembly was thoroughly cleaned and fresh filaments were used. These new filaments were cleaned by heating in vacuo to above 2500°C before use. This

minimized the possibility of cross contamination and helped to remove essentially all traces of natural contamination present on the filaments.

b. Ion Detection

Ion detection was accomplished using a 12-stage Allen type electron multiplier (47Al) with copper-beryllium dynodes, in conjunction with a vibrating reed electrometer and a strip chart recorder. The total gain of the multiplier was about 10,000 for an interdynode potential of about 300 V.

c. Isotopic Analysis

The samples used for measurement contained about 10^{-9} g or less of elements such as cesium, barium, cerium, neodymium and samarium. By suitably adjusting the temperatures of the filaments these elements were ionized off one by one and the isotopic composition measured by averaging the ratios obtained from a large number of spectrograms. Each spectrogram consisted of the result of the forward and backward scanning. This corrects for any small systematic variation in the intensity of the beam during scanning.

The temperatures of the sample and ion filaments ranged from 500°C to 1500°C and 1200 to 2500°C respectively. Cesium and barium were always measured as metal ions, cerium and neodymium as monoxide ions, and samarium as both metal and monoxide ions. The order of appearance of the ions as the filament temperatures were increased was Cs^+, Ba^+, CeO^+, NdO^+ and Sm^+.

The measured intensity ratios were converted into the abundance ratios of the isotopes in fission by correcting for any contamination and any radioactive decay as described below for each element.

d. Systematic Errors in Isotope Abundance Measurements

The two possible systematic errors in abundance measurements are (1) mass discrimination at the electron multiplier and (2) isotope fractionation at the source.

Because of the non-linear nature of the mass dependence of the ion-emission coefficient (γ) of the first dynode of the multiplier, there is a possibility of mass discrimination in isotopic abundance measurements.

Kennett (56K1) reported the absence of mass discrimination effect in the case of the isotopes of krypton and xenon. Irish (56I1) found no systematic variation after a careful study of the abundances of cesium and neodymium isotopes. Farrar (62F1) found no appreciable effect among barium isotopes. Similar conclusions were reached by Clarke (62C1) and Bidinosti (59B2). On the basis of these observations it was assumed that mass discrimination effect was negligible in all cases studied in this work.

Isotope fractionation could arise from the isotope effect in the evaporation of the sample. In an ideal evaporation of a perfectly uniform liquid mixture of isotopes of masses m_1 and m_2, the lighter isotope m_1 will be concentrated in the vapour phase relative to the isotope of mass m_2, and to obtain the true abundance ratio in the liquid, the measured ratio of the heavy to light isotope must be multiplied by $\sqrt{m_2/m_1}$. Nier (38N1) considers it unlikely, however, that the ideal case is approached in the surface ionization method and does not apply any correction for this effect. In addition, evaporation from the sample filament, which takes place at relatively low temperatures in the case of multiple filament sources, is in the form of multi-atomic species (60B1)

and hence the effect should be even smaller. Any fractionation effect should show up as variation in isotopic ratios as the sample is exhausted. No such effect was observed in the present work and hence it was concluded that isotope fractionation in ion production was insignificant.

Measurement of Xenon Ratios

The ratio of xenon isotopes was measured in a gaseous source mass spectrometer described by W. B. Clarke (62Cl). This machine was essentially identical to the solid source machine previously described except that the ion source was of the electron bombardment type (47Nl).

The U_3O_8 samples in this case were irradiated in evacuated quartz vials. After irradiation, the samples were inserted into the sample furnace in the extraction system described by Clarke (62Cl). The system was then evacuated and the sample heated to about 1200°C in the furnace. All gases evolved were collected and purified in a titanium furnace which was heated to 800°C, and the gases were then transferred to a sample tube.

Two methods were used in introducing the sample into the mass spectrometer. In the conventional flow method, the sample was allowed to leak into the ion source at a steady rate and was continuously removed by pumps. In the static method, the rare gas sample was expanded into the mass spectrometer volume which was completely sealed from the pumps.

The ion beam thus produced was analysed in exactly the same way as with the solid samples. Equations to correct for the decay of Xe^{133} are given in Appendix B.

Normalization of the Isotope Ratios

The isotope ratios of various elements measured were normalized with respect to each other to get relative fission yields. This has been achieved by means of an isobaric method as well as by isotope dilution.

a. Isobaric Method

Whenever two elements analysed had an isobar that could be measured, the relative yields of the two could be normalized with respect to each other at that isobar. Thus, xenon and cesium yields could be related to each other by normalizing the two sets of ratios at 133, since both Xe^{133} and Cs^{133} could be measured relative to other isotopes of their respective elements. Similarly cerium and neodymium yields could be normalized at 144 and barium and cerium yields at 140.

b. Isotope Dilution

When the isobaric method of normalization was not possible, isotope dilution was used. In the present work, cesium and neodymium yields were related to each other by means of isotope dilution.

An irradiated uranium sample was divided into two parts. To one was added some isotope dilution solution containing Cs^{133} and Nd^{142} in known ratio. The two parts were separately analysed as usual for cesium and neodymium isotope ratios. The undiluted sample gave isotope ratios in fission, whereas the diluted sample gave ratios which were different in proportion to the amounts of stable isotopes added. It may be seen that

$$\frac{\left(\frac{Cs^{133}}{Cs^{137}}\right)_{dil} - \left(\frac{Cs^{133}}{Cs^{137}}\right)_{und}}{\left(\frac{Nd^{142}}{Nd^{145}}\right)_{dil} - \left(\frac{Nd^{142}}{Nd^{145}}\right)_{und}} = x \left(\frac{Cs^{137}}{Nd^{145}}\right)_{fission}$$

where X is the known ratio of Cs^{133}/Nd^{142} in the isotope dilution solution and the subscripts 'dil' and 'und' refer to the ratios in the diluted and the undiluted samples corrected for any natural Nd^{145}. The only unknown is the ratio of 137 to 145 in fission and hence it can be determined.

It is clear from the above equation that the greater the ratios Cs^{133}/Cs^{137} and Nd^{142}/Nd^{145} in the diluted sample, the less is the error in the value obtained for the abundance ratio of masses 137 and 145 in fission. This fact was exploited in the 'swamping' technique in which the abundances of Cs^{133} and Nd^{142} relative to their other isotopes were increased 10 to 100 fold through isotope dilution. This was achieved through the use of an isotope dilution solution made from analytically pure cesium chloride (isotopically pure in Cs^{133}) and neodymium oxide enriched to 97.45% in Nd^{142} (obtained from the Oak Ridge National Laboratory). The composition of the solution is given in Table III-2.

TABLE III-2

Composition of the Isotope Dilution Solution

Elements	Cesium	Neodymium
Chemical Form Used	CsCl	Nd_2O_3
Isotopic Composition	133 - 100%	142 - 97.45% 143 - 1.04% 144 - 0.89% 145 - 0.21% 146 - 0.26%
Relative Amounts Used (per litre)	0.60214 g (CsCl)	0.18459 g (Nd_2O_3)

IV. RESULTS

In order to obtain relative cumulative yields of the isobaric chains in the fast fission of U^{238}, several corrections must be made to the measured isotope abundance ratios. Firstly, it is necessary to correct for any stable contamination. This correction has been small or negligible in all the cases discussed here except barium. Secondly, if any isotope measured is radioactive or has precursors that are not short-lived as compared to the cooling time, then a decay correction is required. The general method for this correction is discussed in Appendix B. Thirdly, allowance must be made for the independent yields of the isobars appearing later in the chain. In all cases considered in the present investigation, this last correction, assuming equal charge displacement (51G2), was less than a thousandth of the chain yield and, hence, was ignored. Since the irradiations were carried out in cadmium-wrapped capsules, no corrections were required for neutron capture by the fission products. Individual cases are discussed below.

Isotope Abundance Ratios

a. Xenon

Only the abundance ratios of Xe^{133}, Xe^{134} and Xe^{136} were measured in the present work. Both Xe^{131} and Xe^{132} had precursors long-lived in comparison with the cooling time and, under the conditions of the experiments, decay corrections could not be made with the desired accuracy. Natural contamination was quite negligible, as evidenced by

the absence of Xe^{129} which is only produced in fission with a very low independent yield.

The observed abundance at mass 133 included both Xe^{133} and Xe^{133m}. This was corrected to the number of mass 133 atoms produced in fission. The calculation is discussed in Appendix B. Since the samples were irradiated under a cadmium wrap, the amount of Xe^{136} produced by neutron capture in Xe^{135} was negligible.

The relevant data are given in Table IV-1 which includes the results of Wanless and Thode (55W1) for masses 131, 132, 134 and 136. Standard deviations of individual measurements are quoted. The averages of the present measurements and those of Wanless and Thode were taken as the " best " relative yields.

b. Cesium

The measured abundance ratios of cesium isotopes in various samples, the standard deviations, the corrections used and the relative cumulative chain yields obtained from them are given in Table IV-2. Correction for the partial decay of the precursors of Cs^{133} was required only in the case of sample A; all the other samples were cooled long enough to warrant complete decay of the chain into Cs^{133}. The calculations are discussed in Appendix B. Since cesium has only one stable isotope, namely Cs^{133}, it is not possible to decide from one set of measurements alone whether there is any natural contamination. However, the constancy of the ratios in samples which markedly differ in irradiation and cooling time may be taken as sufficient evidence for the absence of contamination from natural cesium.

TABLE IV-1

Abundance Ratios of Xenon Isotopes in the Fast Fission of U^{238}

	131	132	133	134	136
Sample E					
Measured Ratio			0.3459	1.000	0.9077
Standard Deviation			0.0012	-	0.0018
Corrected for Decay[a]			0.868	1.000	0.9077
Sample F					
Measured Ratio			0.2382	1.000	0.9056
Standard Deviation			0.0015	-	0.002
Corrected for Decay[a]			0.844	1.000	0.9056
From Wanless and Thode	0.485	0.711	-	1.000	0.887
Average	0.485	0.711	0.856	1.000	0.897[b]
			0.015	-	0.010

[a]Decay corrections made for the 133 chain using half-life values of 5.27 d for Xe^{133} and 2.35 d for Xe^{133m} (50M1, 52B1).

[b]The average of the value reported by Wanless and Thode (55W1) and that measured in the present work.

TABLE IV-2

Abundance Ratios of Cesium Isotopes in the Fast Fission of U^{238}

	133	135	137
Sample A			
Measured Ratio	0.818	1.125	1.000
Corrected for Decay[a]	1.090	1.125	1.000
Standard Deviation	0.010	0.006	-
Sample B			
Measured Ratio	1.074	1.129	1.000
Corrected for Decay[b]	1.070	1.125	1.000
Standard Deviation	0.016	0.015	-
Sample C			
Measured Ratio	1.089	1.143	1.000
Corrected for Decay[b]	1.076	1.130	1.000
Standard Deviation	0.020	0.018	-
Sample D			
Measured Ratio	1.122	1.160	1.000
Corrected for Decay[b]	1.095	1.132	1.000
Standard Deviation	0.012	0.013	-
Sample D'			
Measured Ratio	1.141	1.189	1.000
Corrected for Decay[b]	1.082	1.128	1.000
Standard Deviation	0.006	0.004	-
Sample G			
Measured Ratio	1.106	1.152	1.000
Corrected for Decay[b]	1.092	1.138	1.000
Standard Deviation	0.009	0.010	-
Weighted Mean	1.086 ± 0.004	1.128 ± 0.003	1.000

[a]Corrected for the incomplete decay of Xe^{133} and Xe^{133m}, using the half-life values 5.27 d and 2.35 d (50M1, 52B1).

[b]Corrected for the decay of Cs^{137}, assuming a half-life of 30.4 years (61F1).

c. Barium

The ratio of Ba^{138} to Ba^{140} was measured in young fission-product samples so that decay corrections for Ba^{140} were small. Even in carefully purified samples, natural contamination could not be avoided. Fortunately, it was possible to correct for this because barium has stable isotopes 136 and 137 which do not appear as fission products, except in small independent yields. Of these, Ba^{136} was preferred as a measure of contamination because of the possibility of small amounts of cesium appearing at mass 137. The measured relative value for Ba^{136}, together with the abundance ratios of isotopes in natural barium, yielded the fractional contamination at mass 138. The corrections involved were fairly large and this is the reason why the error at mass 138 is larger than at any other mass. The measured ratios quoted are the averages of about a dozen spectrograms taken in the period of an hour. Correction for decay during isotopic measurement was not necessary. The data for the barium isotopes are summarized in Table IV-3.

d. Cerium

Cerium ratios were measured in three samples, all of which were cooled long enough to allow the complete decay of Ba^{140}. The only decay corrections were those for the decay of Ce^{144}; the correction factor in this case was about 2.

Correction for contamination was more difficult to make because there is no convenient isotope of cerium which is not produced in fission. However, it is possible to make an indirect estimate of contamination. It is suggested that the natural contamination is small

TABLE IV-3

Abundance Ratios of Barium Isotopes in the Fast Fission of U^{238}

	136	138	140
Sample J			
Measured Ratio	0.0861	1.000	0.1276
Standard Deviation	0.0018	-	0.0017
Corrected for Contamination[a]	-	0.210	0.1276
Corrected for Decay[b]	-	1.005	1.000
Standard Deviation		0.080	-
Sample L			
Measured Ratio	0.0823	1.000	0.1087
Standard Deviation	0.0012		0.0007
Corrected for Contamination	-	0.245	0.1087
Corrected for Decay	-	0.984	1.000
Standard Deviation		0.05	
Weighted Mean		0.992	1.000
Standard Deviation		0.04	-

[a]Using the isotopic abundance ratios for natural barium reported by Nier (38N2).

[b]Correction for the decay of Ba^{140} during irradiation and decay, using a half-life of 12.80 days (51E2).

for two reasons: (1) In the same samples natural contamination of neodymium is only about 1%. (2) The measured ratio of Ce^{140} to Ce^{142} is not very large, even though in natural cerium this ratio is about 8 to 1. The three measured ratios can be reconciled with each other by assuming 7.8%, 11.3% and 4% natural contamination at Ce^{140} in samples C, D and I, respectively. However, in view of the possibility of error in this method of correction, a relatively large error must be attributed to the 140/142 ratio. All the relevant data are tabulated in Table IV-4.

e. Neodymium

The abundance ratios of the isotopes of neodymium were measured in old samples so that decay corrections were not large. Neodymium-143 was always measured in samples which were cooled for more than 150 days to ensure complete decay of Pr^{143}. Neodymium-144 was measured relative to Nd^{143} in samples C' and D which were cooled for 788 and 345 days, respectively. Contamination by natural neodymium, if any, was less than 2%. The existence of stable Nd^{142} which is not produced in fission, except in a small independent yield, made it possible to make contamination corrections quite accurately. The experimental data and the corrections are summarized in Table IV-5.

f. Samarium

Old samples D and I were used to measure the abundance ratios of samarium isotopes 149, 151, 152 and 154. A very small correction was required for the decay of Sm^{151} which has a half-life of 90 years. The abundance of Sm^{150}, relative to that of Sm^{149}, was about 0.005 in both the samples and this could be accounted for by neutron capture in Sm^{149}. The absence of any measurable amount of Sm^{150} suggests that natural contamination was negligible. However, even a small natural contamination at mass 150 would alter the relative abundances of Sm^{152}

TABLE IV-4

Abundance Ratios of Cerium Isotopes in the Fast Fission of U^{238}

	140	142	144
Sample C			
Measured Ratio	1.348	1.000	0.545
Standard Deviation	0.007	-	0.008
Corrected for Decay[a]	1.348	1.000	0.952
Corrected for Contamination[b]	1.25	1.00	0.964
Sample D			
Measured Ratio	1.382	1.000	0.360
Standard Deviation	0.015	-	0.009
Corrected for Decay[a]	1.382	1.000	0.939
Corrected for Contamination[b]	1.24	1.00	0.956
Sample I			
Measured Ratio	1.310	1.000	0.418
Standard Deviation	0.015	-	0.007
Corrected for Decay[a]	1.310	1.000	0.983
Corrected for Contamination[b]	1.26	1.00	0.989
Mean	1.25	1.00	0.970
Estimated Error	0.05	-	0.02

[a]Assuming a 278-day half-life for Ce^{144} (59F2).

[b]Assuming that the fission product Ce^{140} is contaminated by the natural isotope to 7.8%, 11.3% and 4% in samples C, D and I, respectively.

TABLE IV-5

Abundance Ratios of Neodymium Isotopes in the Fast Fission of U^{238}

	142	143	144	145	146	148	150
Sample C							
Measured Ratio	0.0184	1.000		0.8239	0.7402	0.463	0.287
Corrected for Contamination[a]	-	1.000		0.8251	0.7346	0.463	0.2895
Standard Deviation		-		0.015	0.019	0.014	0.009
Sample C'							
Measured Ratio	0.018	1.000	0.880				
Corrected for Contamination[a]	-	0.992	0.864				
Corrected for Decay[b]	-	1.000	0.991				
Standard Deviation	-	-	0.015				
Sample D							
Measured Ratio	0.012	1.000	0.611	0.8227	0.7529	0.459	0.2792
Corrected for Contamination[a]	-	1.000	0.594	0.8243	0.7446	0.459	0.277
Corrected for Decay[b]	-	1.000	0.964	0.8243	0.7446	0.459	0.277
Standard Deviation	-	-	0.030	0.012	0.009	0.007	0.005
Sample G							
Measured Ratio	0.00	1.000		0.820	0.744		
Standard Deviation		-		0.015	0.015		
Sample H							
Measured Ratio	0.00	1.000		0.819			
Standard Deviation		-		0.017			
Weighted Mean		1.000	0.985	0.823	0.744	0.460	0.282
Standard Deviation		-	0.014	0.007	0.007	0.006	0.005

[a]Assuming isotopic abundance data given by Inghram (48I1).

[b]Corrected for the incomplete decay of Ce^{144} using a half-life value of 278 days (59F2).

and Sm^{154} by a few percent. Therefore, even though the measurements involving sample I gave better statistics, sample D was given equal weighting in taking the mean because the latter gave smaller abundance ratios for Sm^{152} and Sm^{154}. The results are shown in Table IV-6. The estimated error takes into account any possible contamination.

g. Rubidium

It is difficult to avoid contamination from natural sources in measuring the abundances of rubidium isotopes in fission, because even the tungsten filament of the mass spectrometer source gives natural rubidium. Whereas, in fission-product samples, Rb^{85} is less abundant than 87, in the natural element it is 2.6 times as abundant; this makes even a small amount of contamination quite noticeable. Since rubidium does not have any other stable isotope not produced in fission, it is not possible to correct for contamination. The two values obtained for the 85/87 ratio in the present work differ by about 12% and it is obvious that at least one of them is contaminated. However, it is suggested that the amount of contamination is small on two grounds: (1) In the same samples, natural cesium was absent. (2) The ratio of Rb^{85} to Rb^{87} is low. The lower value may be taken as close to the true value. The relevant data are shown in Table IV-7.

h. Strontium

Only one measurement was made on strontium isotopes. Contamination correction at mass 88 was not high and could be made rather accurately using the abundance of Sr^{86}, which is not produced in fission in any significant yield. The decay correction for Sr^{89} is large and this makes the relative abundance of Sr^{89} susceptible to a larger error. Table IV-8 summarizes the available data.

TABLE IV-6

Abundance Ratios of Samarium Isotopes in the Fast Fission of U^{238}

	149	151	152	154
Sample D				
Measured Ratio	1.000	0.5035	0.299	0.122
Standard Deviation	-	0.015	0.010	0.006
Corrected for Decay[a]	1.000	0.507	0.299	0.122
Sample I				
Measured Ratio	1.000	0.487	0.331	0.146
Standard Deviation	-	0.006	0.005	0.006
Corrected for Decay[a]	1.000	0.490	0.331	0.146
Mean	1.000	0.50	0.315	0.134
Estimated Error	-	0.01	0.015	0.010

[a]Decay of Sm^{151} is corrected for, assuming a half-life of 90 years.

TABLE IV-7

Abundance Ratios of Rubidium Isotopes in the Fast Fission of U^{238}

	85	87
Sample C		
Measured Ratio	0.4424	1.000
Standard Deviation	0.0084	-
Corrected for Decay[a]	0.54	1.00
Sample D		
Measured Ratio	0.3936	1.000
Standard Deviation	0.0055	-
Corrected for Decay[a]	0.48	1.00
Recommended Value[b]	0.48	1.00

[a]81% of 4.4-hr Kr^{85m} decays to Rb^{85} and the other 19% through 10.6-y Kr^{85} (60W1).

[b]Assuming that the smaller value is free of contamination correction.

TABLE IV-8

Abundance Ratios of Strontium Isotopes in the Fast Fission of U^{238}

	86	88	89	90
Sample C				
Measured Ratio	0.0336	0.9393	0.0416	1.000
Standard Deviation	0.0008	0.0186	0.0016	-
Corrected for Contamination[a]	-	0.658	0.0416	1.000
Corrected for Decay[b]	-	0.650	0.796	1.000
Estimated Error	-	0.02	0.04	-

[a]Assuming the natural abundances of isotopes 88 and 86 as 82.56% and 9.83%, respectively (57S2).

[b]The half-lives of Sr^{89} and Sr^{90} were taken as 51.8 d and 27.7 y, respectively (59F3, 55W2).

Isotope Dilution

In samples K and M, which were used for isotope dilution, the decay of Pr^{143} was not complete. Hence, Nd^{142} was measured relative to Nd^{145} rather than Nd^{143}. The accuracy of the method has been greatly improved by " swamping" Cs^{133} and Nd^{142}. The latter was possible through the use of neodymium enriched to 97.45% in 142. Further, because of the swamping, a few percent contamination of Cs^{133} in the original sample would make negligible difference. Neodymium-142 was present only in insignificant amounts in both the samples. The relevant data are given in Table IV-9.

Since the degree of " swamping" was greater in sample M than in sample K, the value obtained from it should be given more weight than is suggested by statistical errors. Hence it was decided to average the two values rather than take a weighted mean. The quoted error is an estimate.

Relative Yields

The abundance ratios of the various isotopes of the elements xenon, cesium, barium, cerium, neodymium and samarium are combined together to give relative fission yields in the fast fission of U^{238}.

By equating the yields of Xe^{133} and Cs^{133}, the xenon and cesium ratios are normalized with respect to each other. Thus we get the relative yields from masses 131 to 137. Similarly, barium and cerium ratios are normalized at mass 140, and cerium and neodymium ratios at mass 144. Samarium ratios are related to neodymium ratios by adjusting the yield for mass 149 to the mean of the Nd^{148} and Nd^{150} values. Thus yields for masses 138 to 154 are obtained relative to each other. The isotope dilution data relates the yields at masses 137 to 145. With this it became possible to get the yields of all the heavy masses studied relative to each other. The data are summarized in Table IV-10.

TABLE IV-9

Data on Isotope Dilution

	Sample K	Sample M
Ratio of Cs^{133} to Cs^{137} in the isotope diluted sample[a]	19.50 ± 0.06	44.09 ± 0.40
Ratio of Cs^{133} to Cs^{137} in the undiluted sample	1.09 ± 0.01	1.14 ± 0.04
Hence ratio of natural Cs^{133} added to Cs^{137} from fission (R_{Cs})	18.41 ± 0.06	42.95 ± 0.40
Ratio of Nd^{142} to Nd^{145} in the isotope diluted sample[b]	7.822 ± 0.025	18.54 ± 0.14
Ratio of 142 to 145 in the undiluted sample	0.0	0.0
Hence ratio of natural 142 added to the fission 145 (R_{Nd})	7.822 ± 0.025	18.54 ± 0.14
Ratio of Cs^{133} to Nd^{142} in the isotope dilution solution (X)	3.2332	3.2332
Ratio of fission 137 to fission 145 ($R_f = (R_{Nd}/R_{Cs}) \times X$)	1.374 ± 0.007	1.396 ± 0.022
Mean Value of R_f	1.385 ± 0.010	

[a]Corrected for the decay of Cs^{137}.

[b]Corrected for the small contamination of mass 145 arising from the spike.

TABLE IV-10

Relative Yields of the Heavy Mass Fission Products in the Fast Fission of U^{238}

	Xenon	Cesium	Barium	Cerium	Neodymium	Samarium	From Isotope Dilution	Relative Yields
131	0.485							0.582
132	0.711							1.249
133	0.856	1.086						1.504
134	1.000							1.757
135		1.128						1.562
136	0.897							1.576
137		1.000					1.385	1.385
138			0.992					1.531
140			1.000	1.25				1.543
142				1.000				1.234
143					1.000			1.215
144				0.970	0.985			1.197
145					0.823		1.000	1.000
146					0.744			0.904
148					0.460			0.559
149						1.000		0.451
150					0.282			0.343
151						0.500		0.225
152						0.315		0.142
154						0.134		0.060

Absolute Yields

In order to obtain absolute yields, the relative yields of the heavy mass fission products were normalized such that they add to 100%. In the mass range from 131 to 154, only four relative yields were not measured in the present work, viz., those of masses 139, 141, 147 and 153. These were obtained by interpolation. Using radiochemical data for the yields of Sb^{127} and Eu^{156}, it was possible to extrapolate the mass-yield curve to either side and thus obtain relative yields of the mass numbers 128, 129, 130 and 155. Estimates were made of the total yields of the mass numbers 120 to 126, as well as 157 and above, through the use of available radiochemical data and extrapolation. The absolute yields thus obtained, along with relative yields, are given in Table IV-11. The fission yields are plotted against mass numbers in Fig. IV-1.

TABLE IV-11

Relative and Absolute Yields in the Fast Fission of U^{238}

	Relative Yields	Absolute Yields
120 to 126[a]	0.015	0.06
127[b]	0.032	0.13
128[c]	0.140	0.56
129[c]	0.290	1.16
130[c]	0.510	2.03
131	0.852	3.40
132	1.25	4.98
133	1.504	6.00
134	1.757	7.00
135	1.562	6.23
136	1.576	6.28
137	1.385	5.52
138	1.531	6.10
139[c]	1.535	6.12
140	1.543	6.15
141[c]	1.395	5.56
142	1.234	4.92
143	1.215	4.84
144	1.197	4.77
145	1.000	3.99
146	0.904	3.60
147[c]	0.710	2.83
148	0.559	2.23
149	0.451	1.80
150	0.343	1.37
151	0.225	0.90
152	0.142	0.57
153[c]	0.093	0.37
154	0.060	0.24
155[c]	0.032	0.13
156[b]	0.019	0.08
>156[a]	0.025	0.10
	Total	100.02

[a]Estimate.

[b]Radiochemical yield taken from (60K1).

[c]Obtained by interpolation and extrapolation.

Fig IV-1

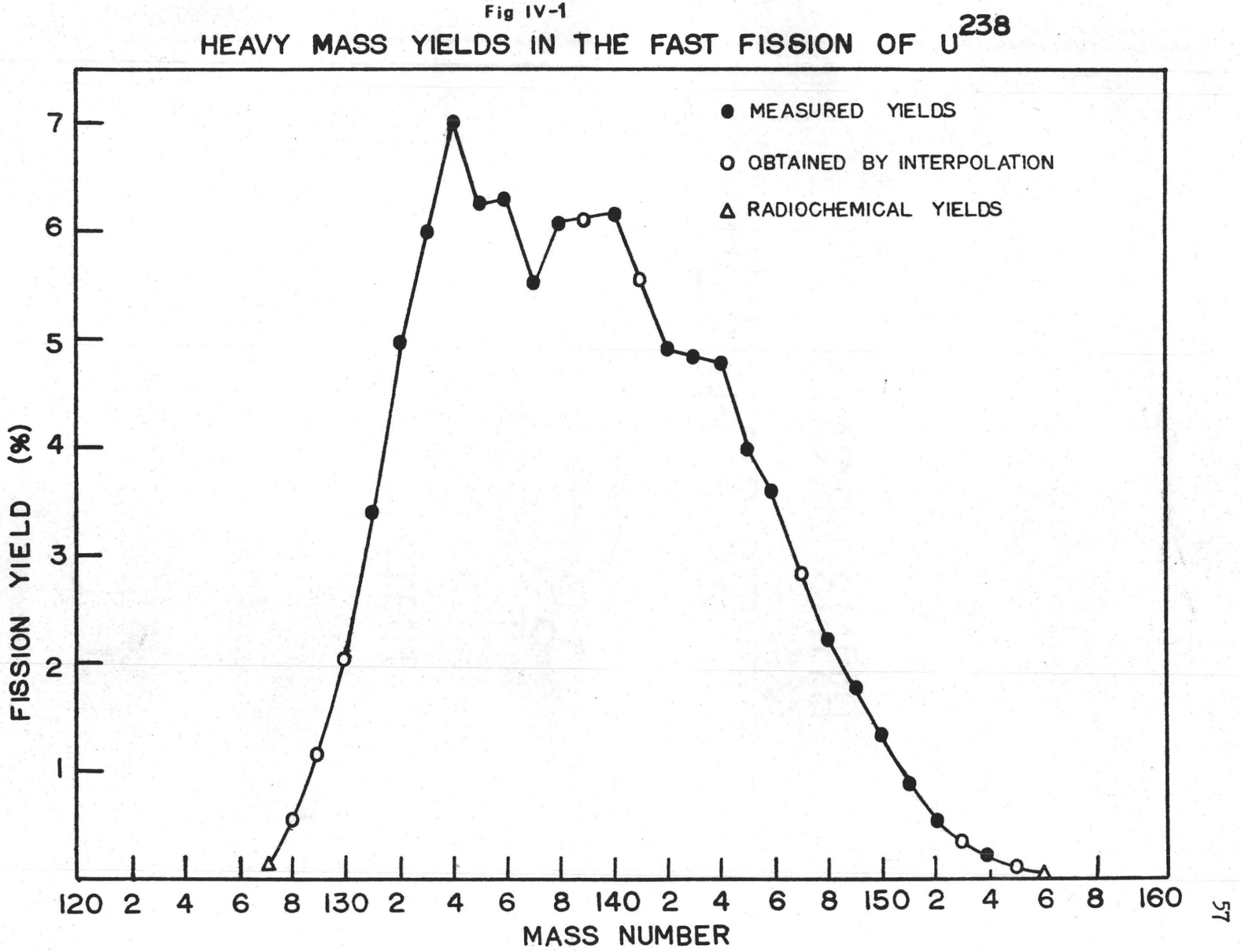
HEAVY MASS YIELDS IN THE FAST FISSION OF U238
MEASURED YIELDS
OBTAINED BY INTERPOLATION
RADIOCHEMICAL YIELDS
FISSION YIELD (%)
1
2
3
4
5
6
7
120 2 4 6 8 130 2 4 6 8 140 2 4 6 8 150 2 4 6 8 160
MASS NUMBER

V. DISCUSSION

Discussion on Errors

The relative values of cumulative chain yields obtained through isotopic abundance measurements suffer from two sources of error: statistical and systematic errors in the measurements and errors arising from corrections for decay and contamination. The statistical errors have, in general, been about 1%, as is evident from the standard deviations quoted with individual measurements. Systematic errors have also been small; they have already been discussed in Chapter III. The other errors depend on individual cases.

There was no correction for natural contamination involved in the case of xenon ratios. Only Xe^{133} required decay correction. The uncertainties in the half-lives of Xe^{133} (5.27 d) and Xe^{133m} (2.35 d) are taken into account in the 2% error quoted for the relative yield of mass 133.

Natural contamination was absent in the cesium samples as well. This is seen from the constancy of the 133/137 ratio in samples having different irradiation and cooling history. Only in sample A was the 133 chain incompletely decayed to Cs^{133}; even there the decay correction was small. The cesium ratios are thus expected to be reliable to about 1%.

Corrections for decay and contamination were large in the case of the Ba^{138}/Ba^{140} ratio. In the two samples analysed, about 70 to 80% of the Ba^{138} present came from natural contamination. The correction

factor for the decay of Ba^{140} was about 2 in both the samples, but the error involved in this is comparatively small. The 138/140 ratio is believed to have an uncertainty of about 5%.

The most widely accepted value for the half-life of Ce^{144} is about 285 days (56S2). However, Fickel (59F2) found it necessary to use a shorter half-life of 278 days in order to reconcile the abundance ratios of cerium isotopes in fission measured after widely different cooling periods. This value of the half-life was used in the present work also. The error introduced through the uncertainty in half-life is, however, not more than about 1%. Contamination correction at mass 140 was less accurate. This correction was made by assuming a contamination of 7.8% in sample C, 11.3% in sample D, and 4% in sample I. An error of 5% has been attributed to the 140/144 ratio. Since the true ratio in fission should be at least as low as the lowest measured ratio, the error cannot be more in the upper limit. If the true ratio is more than 5% less, then the three sets of values become less consistent with each other.

The contamination correction in the case of the neodymium ratios was quite small. Decay correction affected only mass 144 and is expected to be accurate to about 1%. Thus the relative yields of these mases are believed to be reliable to about 1 to 2%.

Very little correction was required in the case of the samarium ratios. The errors estimated on the basis of the agreement between the two sets of data are about 2% at mass 151, 5% at mass 152, and 7% at mass 154. The errors at these masses are relatively large for two reasons: (1) The absolute yields of these masses are small and hence the abundance of samarium isotopes in fission-product samples are low. (2) In natural

samarium, isotopes 152 and 154 occur in high abundances, so even when there is no measurable amount of Sm^{150} present there could be some contamination at masses 152 and 154.

The abundance ratio of Rb^{85} and Rb^{87} may be taken as an upper limit value. It is suggested that contamination is not large in this case and the recommended value is close to the true value, since cesium contamination was absent in the same samples.

Among the strontium isotopes, only 88 is affected by contamination correction; here the total error arising from both measurement and correction is under 3%. The decay correction for Sr^{89} was made by using a half-life of 51.8 days obtained by Fickel and Tomlinson (59F3). The correction factor is large and this makes the abundance ratio uncertain to about 5%. Only a very small decay correction was required in the case of Sr^{90}.

The absolute yields obtained in this work are subject to errors arising from three additional sources: isotope dilution, isobaric method of normalization of relative yields, and the normalization of relative yields to 100%.

The cumulative yield of Cs^{137} was measured relative to that of Nd^{145} by isotope dilution in two different samples and the values agreed to within 1.5%.

The error in the isobaric method of normalization depends on the reliability of the relative yields of the isobars concerned. The normalization of xenon and cesium isotope ratios at mass 133 and cerium and neodymium isotopes at mass 144 are expected to be reliable to about 2.5%, whereas that of barium and cerium isotopes at mass 140 may have an error of about 5%. This makes the absolute yield at mass 138 uncertain to about 7%.

The normalization of the relative yields to 100% contributes a relatively smaller error. The only interpolated yields are those at masses 128, 129, 130, 139, 141, 147, and 153. Of these, all except those at masses 139 and 141 must be considered good estimates because they fall in regions where the mass-yield curve is relatively smooth; moreover, they are all low yields and add up to only 7% of the total. Even if the yields at 139 and 140 are in error by as much as one fission-yield percent, the normalization procedure does not introduce more than 2% error.

It is difficult to combine all these errors statistically and quote probable errors for the absolute yields. However, we estimate that the measured yields quoted in Table IV-11 are reliable to within 3% in all cases except at masses 138, 140, 152 and 154. The uncertainties in the yields are about 5% at masses 140 and 152, and 7% at masses 138 and 154.

Comparison of Present Results With Other Available Data

In comparing the fission yields obtained in the present work with other data available in the literature, one must keep two things in mind: (1) The radiochemical measurement of relative yields suffers from an error of over 10%. (2) Because of the fact that only a few yields had been measured, the normalization of the yields could be seriously in error. Even in Katcoff's tabulation, which included the mass spectrometric data of Wanless and Thode (55W1) and Tomlinson (60T1), the yields of masses 138, 139, 141, 142, 143, 145, 146, 148, 150, 151, 152, and 154 were missing. These make up about half the total yields of the heavy mass fission products. Since Katcoff was compelled to depend on interpolation for all these yields, his normalization is likely to be in error.

The radiochemical yield measurement of those nuclides which are produced in large yields in the fast fission of U^{238} was carried out by Keller et al (54K1) and these authors quote an error of more than 10% in the relative yields. The agreement between the radiochemical yields as normalized by Katcoff and the absolute yields quoted in the present work is within 10% at mass numbers 140, 144, 147, 149 and 153. The radiochemical yield of Cs^{137} is particularly high. This is understandable because, in the radiochemical method, the yields of long-lived nuclides are particularly susceptible to error. In addition, Keller et al used a half-life of 33 years for Cs^{137} in converting count rate into numbers of atoms. Since the currently accepted value for Cs^{137} half-life is 30.4 years (61F1), this introduces an additional systematic error of about 10%.

The mass spectrometric data of Wanless and Thode for the relative yields of xenon isotopes have been incorporated into the present work. The absolute yields of masses 131, 132, 134 and 136, as given by Katcoff, are within 5% of the values obtained in the present work.

Interpretation of Results

It is fairly well established that the sequence of events in the low energy fission of a heavy nucleus is as follows:

1. The compound nucleus splits into two fragments.
2. The fragments emit prompt neutrons and gamma rays.
3. The de-excited fragments undergo beta decay along the isobaric chain towards stability.
4. The total energy release for certain fission-product nuclei undergoing beta decay is greater than the

neutron binding energy of the daughter nucleus. In such a case, delayed neutrons may be emitted with an observed decay rate that approximates that of the precursor.

The emission of beta and gamma rays does not change the mass numbers of the fragments. The cumulative chain yields obtained are the integrated yield of the total chain and, hence, the data is already corrected for beta decay. It would be interesting to investigate the irregularities brought about in the mass distribution through neutron emission and determine the nature of the prompt mass distribution.

a. Delayed-Neutron Emission

It is not easy to correct accurately for the effects of delayed-neutron emission because of the inadequate information available on the yields and precursors of delayed-neutron emitters. The data on delayed-neutron emitters have been summarized in several reviews (56K2, 56C1, 58M2). Keepin and co-workers at Los Alamos have done extensive work in this field and the following discussion is based mainly on their results (62K1).

The Los Alamos group made use of high intensity irradiations and obtained good counting statistics in following delayed-neutron decay. Measured decay curves were analysed into a series of exponential decay groups by an iterative least-square method coded for high-speed digital computation. It was found that six exponential periods were necessary and sufficient for optimum least-square fit to the decay data. A summary of their results for the fast fission of U^{238} is given in Table V-1.

Total delayed-neutron emission yields have been measured by several workers. For the fast fission of U^{238} the weighted average of the various measurements is 3.98 per 100 fissions, while the Los Alamos

TABLE V-1

Delayed-Neutron Periods and Abundances in the Fast Fission of U^{238}

Group Index	Half-Life	Relative Abundance	Yield Per 100 Fissions
1	52.38 ± 1.29	0.013 ± 0.001	0.052
2	21.58 ± 0.39	0.136 ± 0.002	0.55
3	5.00 ± 0.19	0.162 ± 0.020	0.65
4	1.93 ± 0.07	0.388 ± 0.012	1.55
5	0.490 ± 0.023	0.225 ± 0.013	0.9
6	0.172 ± 0.009	0.075 ± 0.005	0.3
		Total	4.00

group gives the value 4.12. We have chosen to use a delayed-neutron yield of 4 per 100 fissions and have worked out the yields of the various groups of delayed-neutrons given in column IV of Table V-1.

Precursor assignment is less definite. The 54.5-sec period is known to be that of Br^{87}. The 22-sec period is complex, being made up of 16.3-sec Br^{88} and 22.4-sec I^{137}. In U^{235} these appear in the ratio of approximately 2 to 3. Iodine-138 and some isotopes of bromine and rubidium make up the 5-sec period. The 2-sec period is also complex and involves I^{139}, some isotopes of bromine and krypton, and maybe some isotopes of cesium, antimony or tellurium. The available information on precursors is tabulated in Table V-2.

The delayed-neutron yields from various precursors will be different in the case of U^{238} fission from the values given in Table V-2 for U^{235} fission. However, the yields in U^{235} may be used in estimating those in U^{238} by assuming that yields are greater (or smaller) in proportion to the change in the cumulative yield of the chain up to (and including) the precursor of interest. The cumulative yield of a chain up to a given precursor, which is the sum of the independent yields of all the members of the chain up to the precursor, may be estimated by using the hypothesis of equal charge displacement (51G2).

The neutron yields calculated in this manner for the various precursors making up a given complex period, however, do not add up to the value quoted in Table V-1. For example, the calculated yields of delayed neutrons from Br^{88} and I^{137} are 0.1 and 0.3 respectively, which give a total of 0.4 delayed neutrons per 100 fission, whereas the value associated with the 22-sec period is 0.55. The calculated values were, therefore, used only as a guide in making the following estimates of

TABLE V-2

Delayed-Neutron Precursors

Group Number	Precursor Assignment[a]		Yield in U^{235} Fission (Neutrons/100 Fissions)
1	54.5 sec	Br^{87}	0.058
2	24.4s	I^{137}	0.22
	16.3s	Br^{88}	0.157
3	6.3s	I^{138}	0.103
	4.4s	$Br^{(89)}$	0.298
	6s	$Rb^{(93,94)}$	0.001
4	2.0s	I^{139}	0.084
	(1.6 - 2.4s)	(Cs, Sb or Te)	0.206
	1.6s	$Br^{(90 - 92)}$	0.236
	1.5s	$Kr^{(93)}$	0.007
5	0.5s	(I^{140} + Kr?)	-
6	0.2s	(Br, Rb, As?)	-

Table taken from Ref. (62K1).

[a]Tentative or uncertain assisgnments given in paranthesis.

the distortions in the mass distribution brought about by delayed-neutron emission. The delayed-neutron yields from masses 137, 138 and 139 are estimated at about 0.35, 0.15 and 0.25 units (percent cumulative yield) respectively.

The mass-yield curve corrected for delayed-neutron emission is shown in Fig. V-1. In making the correction, we have arbitrarily placed the yield of mass 139 at 6.20 because it was only an interpolated yield and would probably have been found depressed if measured. The yield at mass 138 has been reduced by 0.1 units and that at 136 by 0.35 units, while the yield of mass 137 was increased by 0.2 units. These corrections have removed most of the irregularities in the mass distribution between masses 136 and 139.

b. Prompt Neutron Emission

It is interesting at this point to compare the fine structure in the mass distribution of fission products from U^{238} with those from the fission of U^{233} and U^{235}. We choose to compare the mass-yield curves after correction for delayed-neutron emission. In Fig. V-2 the three curves are superimposed on each other. The U^{235} data are from Farrar and Tomlinson (62F3) and the U^{233} data from Bidinosti, Irish and Tomlinson (61B2). The following features are noteworthy:

1. All three curves seem to coincide at the low mass end.
2. At the heavy mass end, the U^{238} curve is wider than the other two by about 1 to 2 mass units.
3. The fine structure in the region of high yield suggests the existence of three maxima in all the cases. The peak at mass 134 is common, even though it is highest for U^{235} and lowest for U^{233}. The second peak is in

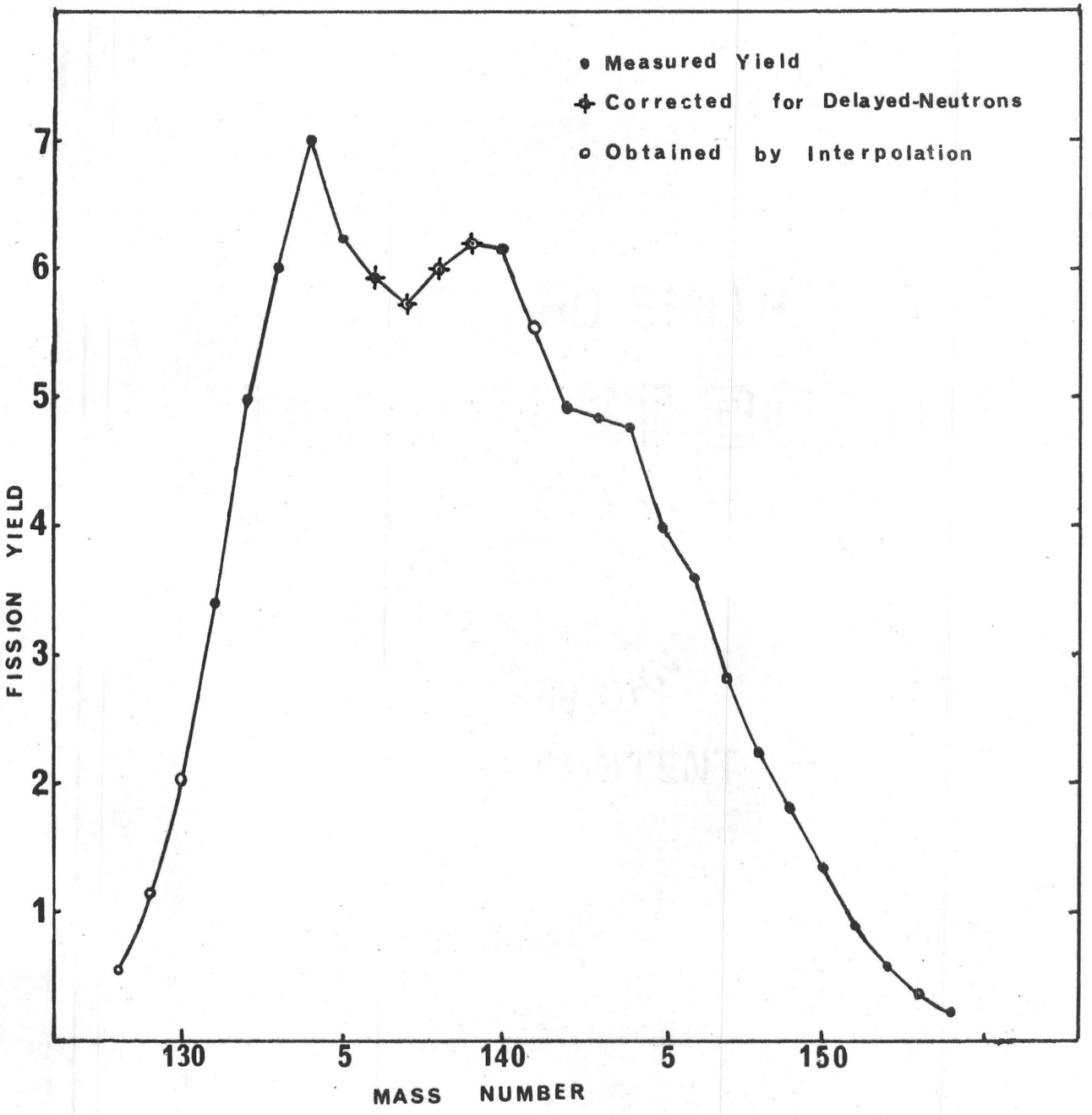

FIG. V-1: Heavy Mass Yields After Correcting for Delayed-Neutron Emission

FIG. V-2 FISSION YIELDS OF U^{233}, U^{235}, U^{238}

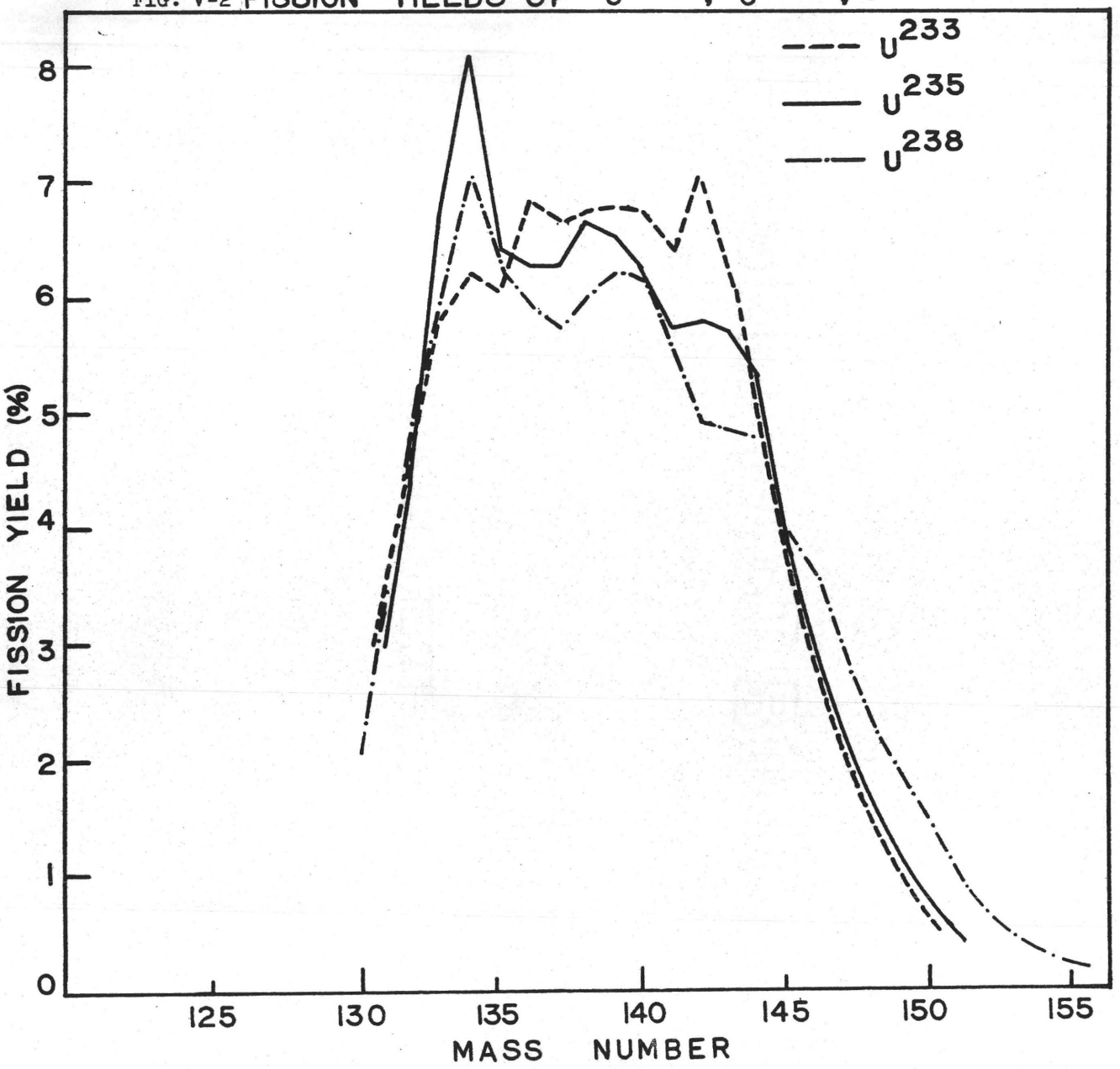

the 136-140 mass region; at 138 in the U^{235} curve; at about 139-140 in the case of U^{238}, and less definite in the U^{233} curve. The third peak is at 142 in the case of U^{233}, at about 142-143 in U^{235} and at about 144 in the U^{238} curve.

Several authors have attempted to explain the fine structure in the mass-yield curve around mass 134. Glendenin (49G1) proposed that fission products with 83 neutrons would tend to 'boil off' an extra neutron and reach the shell configuration of 82 neutrons. This would increase the yield at mass 134 at the expense of that at mass 135. Pappas (53P1) extended the Glendenin hypothesis to include neutron boil off from nuclides with 85, 87 and 89 neutrons. However, the hypothesis requires that any increase in the yields of 134, 136 and 138 mass chains over those expected from the 'smooth curve' should be counterbalanced by the dips at masses 135, 137, and 139, respectively. These dips were not observed in the mass spectrometric studies made by several workers (50W1, 55P1, 62F2).

Wiles et al (53W1) postulated that high yields near mass 134 arise from a preference in the fission act for fragments with 82 neutrons. A natural corollary of this postulate is that the anomalous yields of 82-neutron fragments must be reflected in the yields of the complementary light fragments. The observation by Glendenin, Steinberg, Inghram and Hess (51G1) that Mo^{100} is produced in unusually high yield in U^{235} lent support to the Wiles hypothesis; for masses 100 and 134 are complementary after the usual two neutrons are emitted. However, the subsequent measurements by Tomlinson and co-workers (59F1, 61B2) of the mass distribution in

the fission of U^{233} and Pu^{239} show that, in these cases also, there is a maximum at mass 100 even though masses 100 and 134 are no longer complementary.

Fickel and Tomlinson (58F1) have suggested that an increased stability of primary fragments in the region of 50 protons and 82 neutrons may cause a decrease in neutron emission in the mass 134 region. Such a decrease would cause a bunching up of yields such as that found in the 131-136 mass range. This may be illustrated by means of a fictitious example. If the fission fragments with masses 136 and above emitted an average of 1.5 neutrons and mass 135 emitted only one neutron, then the final yield at mass 134 would be made up of contributions from prompt fragments of masses 135 and 136. Hence the 134 yield would be abnormally high. The net effect of such neutron emission would be to narrow the mass-yield curve of the heavy mass fission products in relation to that of the light mass products. In fact, it was the observation of this effect which led Fickel and Tomlinson to the above explanation of the fine structure at mass 134.

The direct measurement of prompt neutron yields from fission fragments has shed much light on the origin of the fine structure. Strong variation of neutron yield with fragment mass was first observed by Fraser and Milton (54F1). After studying the neutron emission in U^{233} fission, these authors came to the conclusion that neutrons are emitted preferentially by the heaviest light fragments and by the heaviest heavy fragments. More accurate measurements, using improved techniques, were carried out by Whetstone (59W1) on the spontaneous fission of Cf^{252}. He concluded that neutron yield increased with the mass of the emitting fragment in both the light and heavy mass groups, and showed a striking discontinuity

in the mass region corresponding to symmetric fission. Similar conclusions were arrived at by Apalin and co-workers (60A1), who investigated the neutron emission in the thermal neutron fission of U^{235}.

It is obvious that variation of prompt neutron yields with fragment mass would introduce irregularities in the mass-yield curve. Thus the prompt yield distribution will not correspond exactly to the cumulative yields. The time-of-flight method has yielded the most accurate measurements on prompt yields. The data of Milton and Fraser (62M1) and Stein (57S1) show that the prompt yield curve is much smoother than the cumulative (final) yield curve for the neutron fission of U^{233} and U^{235}.

The most detailed analysis of the irregularities brought about by prompt neutron emission on the mass distribution was carried out by Terrel (62T1). He combined the best available data on prompt (initial) yields and cumulative (final) yields to get the prompt neutron distributions for several fissioning nuclides. The results, which are similar to the experimental measurements discussed above, are shown in Fig. V-3 and Fig. V-4. One of the important conclusions of Terrel's analysis is that slight changes in neutron emission probabilities from one fragment to the next can produce pronounced fine structure in the cumulative (final) mass-yield curve, even though the prompt mass distribution is relatively smooth. In particular, the sharp peak in the mass-yield curve at mass 134 is easily accounted for by a slight change in the slope of the prompt neutron distribution at about mass 136.

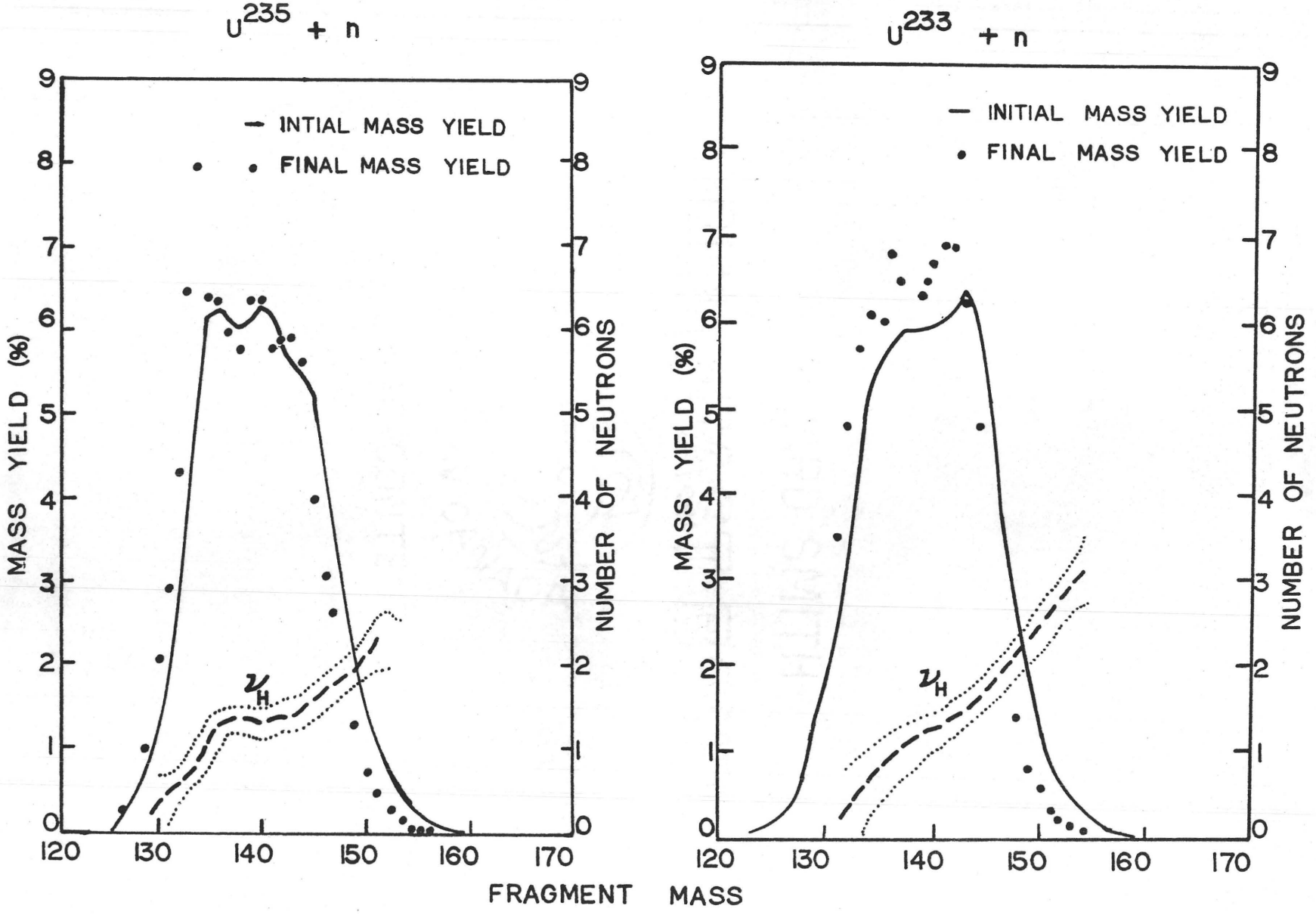

FIG. V-3: Prompt Neutron Yields and Mass-Yield Curves

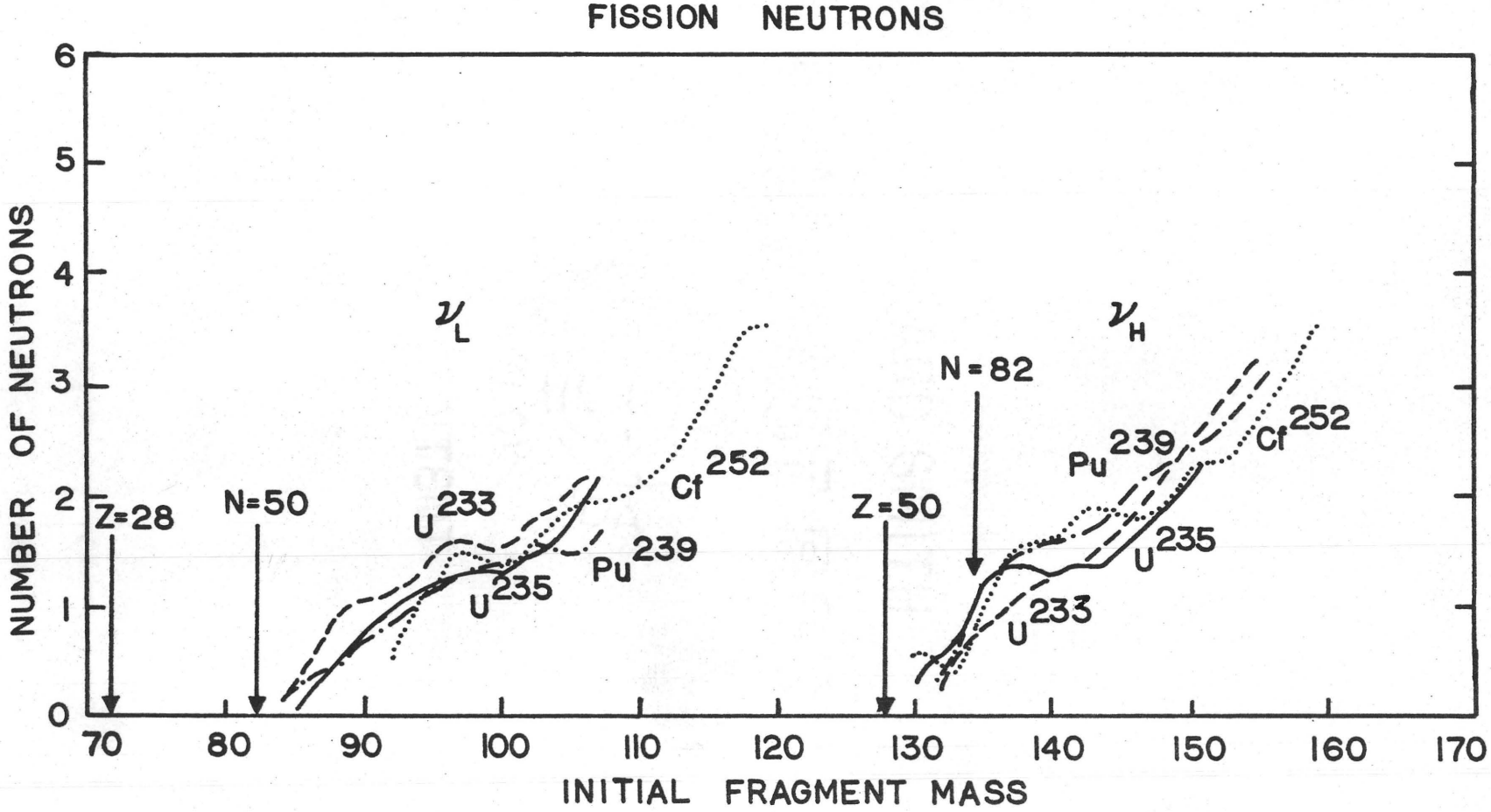

FIG. V-4: Prompt Neutron Yields for Various Fissioning Nuclides

c. Fine Structure in the Prompt Mass Distribution

Whether the prompt mass distribution has any fine structure is a matter of considerable interest. According to Thomas and Vandenbosch (64T1) the fine structure in the prompt yield curve is related to the structure in the mass surface for even-even fragments. Using the semi-empirical mass equations, they pointed out that the total energy release in fission is the sum of the changes in the Coulomb, surface and asymmetry terms and a term Δ representing the shell and pairing effects. While most of the energy released comes as the difference between the Coulomb and surface terms, the asymmetry term causes oscillations. The term Δ has two effects: (1) It causes divisions leading to fragments with closed shells to be more energetically favourable than would be otherwise expected. (2) It causes the energy release for odd mass fragments to be depressed somewhat below that for even-even fragments. After investigating the thermal neutron fission of U^{233}, U^{235} and Pu^{239}, these authors came to the conclusion that there is a correlation between the structure in the prompt mass distribution and the maximum energy release. The energy release for the even-even products is greater than for the odd mass products, so the structure is determined by the mass surface for the even-even products. The structure for the even-even products has a periodicity of about 5 mass units because the mass number of the most stable nuclides for a given Z changes about 2.5 units for a unit change in Z. Thomas and Vandenbosch argue that this accounts for the three maxima found in the prompt fission yield curves at about masses 135, 141 and 146. If this were the only source of fine structure in the prompt mass distribution, then there would be no fine structure in the case of the neutron-induced fission of U^{238} because every even-A fragment would have an odd-A complement.

Time-of-flight measurements indicate the existence of fine structure in the prompt mass distributions for the thermal neutron fission of U^{233} and U^{235}; the heavy fragment distribution shows three maxima at about masses 135, 140 and 144-145 (see Fig. V-3). No time-of-flight measurements have been reported on the neutron-induced fission of U^{238}. Two ion chamber studies have been reported--one by Henkel (62H2) and the other by Baranov, Protopopov and Éĭsmont (61B3). Both made use of the back-to-back ionisation chamber. Henkel used 1.5 Mev neutrons, and Baranov et al 3 Mev neutrons, to induce fission. Their results are shown in Fig. V-5 along with the cumulative yields obtained in the present work. The mass distributions show only a single maximum and are wider than the cumulative (final) yield curve. Since neutron emission can in no way account for a prompt mass distribution that is wider than the cumulative mass distribution at the low mass end, the prompt distributions must be considered seriously in error. The error probably arises from the fact that these investigators used thick targets to get better counting statistics. It is evident that these prompt mass distributions cannot be used in any discussion of the fine structure without additional information.

There are two possible ways in which we can attempt to find out if there is any fine structure in the prompt mass distributions from the fast neutron fission of U^{238}. One may assume a reasonable neutron yield distribution and, starting from the measured cumulative yields, work out the prompt mass-yield curve. One may also start by assuming a smooth prompt mass distribution without any fine structure and find out whether the calculated neutron distribution is reasonable as compared to the known distributions in other cases.

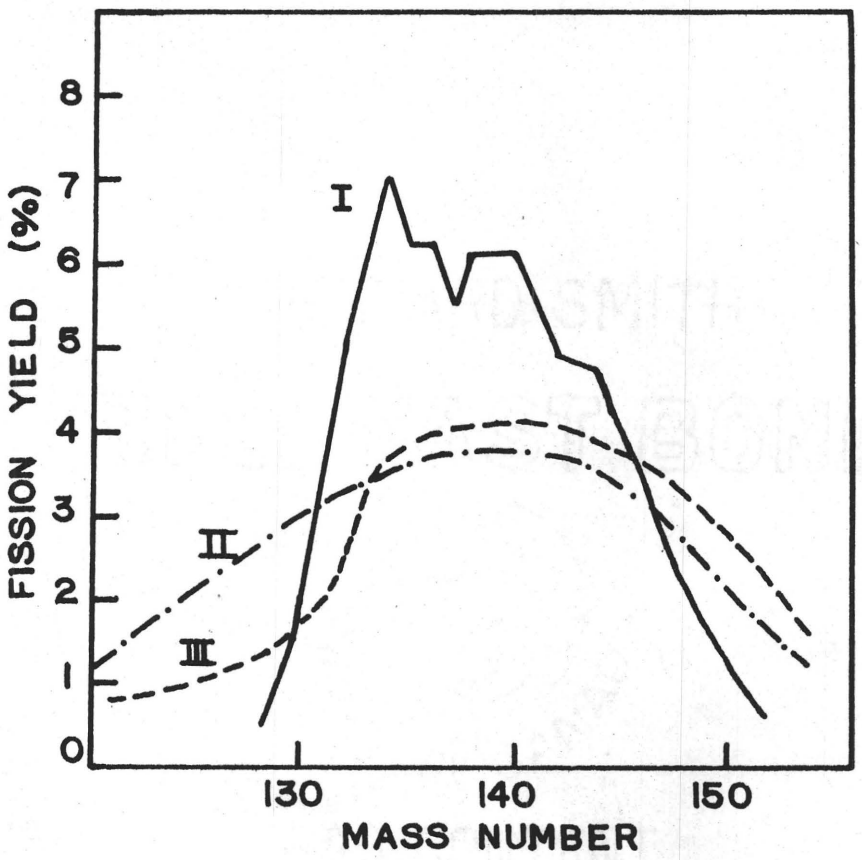

FIG. V-5: A Comparison of the Available Data on the Prompt Mass Distribution in the Fast Neutron Fission of U^{238} With the Cumulative Yields Obtained in the Present Work

I. The cumulative mass-yield curve
II. Prompt mass distribution from Henkel's data (62H2)
III. Prompt mass distribution from the data of Baranov et al (61B3)

A careful examination of the neutron distributions for various fissioning nuclides shows that as the neutron-to-proton ratio of the fissioning nuclide increases, the horizontal portion in the curve becomes longer (see Fig. V-4). This might perhaps suggest that the neutron yield curve in the case of U^{238} has a longer horizontal region starting at mass 136 than in the case of U^{235}. Whether one assumes a distribution like this, or a universal function like the one suggested by Terrel (62T1), it turns out that the prompt mass distribution obtained by correcting the cumulative mass-yield curve for neutron emission shows three maxima; in particular, the two maxima at about masses 135 and 140 are unmistakable.

For each reasonable prompt mass distribution with a single maximum, a neutron distribution consistent with the observed cumulative yields may be obtained. It is characteristic of these, however, that considerably more structure in the neutron distribution is found than in any of the experimental curves obtained for other nuclides.

Neither of the above arguments can be considered conclusive, but, in view of the general similarity of the cumulative mass-yield curve of U^{238} to those of U^{233} and U^{235}, both of which show three maxima in their prompt mass distributions, it is probable that U^{238} will also show three maxima in the distribution of the prompt fragments. If this is true, it is against the prediction of the Thomas and Vandenbosch postulate. In the following discussion we try to speculate on the origin of the three maxima in the heavy fragment mass distribution in terms of a modified Whetstone model (59W1).

One can imagine the scission configuration to consist of two deformed spheres of unequal sizes connected by a neck. The bigger lobe may be considered to be made up of the Z = 50 and N = 82 shell (A = 132)

and the smaller lobe of the N = 50 shell ($A \approx 90$). The most probable division would then be at the middle of the neck. This makes the maximum in the distribution of heavy mass fragments around mass 140, in the case of U^{235} fission, and around mass 146, in the case of Cf^{252}, which is consistent with experimental observation. In the original Whetstone model, symmetric fission corresponds to the scission at the end of the neck. In the present model, the heavy lobe contains 132 nucleons and hence symmetric fission would require the break-up of a shell; this would be energetically unfavourable. It would be expected that the probability of fission would decrease as the point of scission moves away from the centre of the neck to either lobe, except at some point close to either neck where the scission configuration would contain an undeformed shell. The favouring of the latter modes of fission would modify the mass distribution, giving rise to two maxima in addition to the one corresponding to the scission at the centre of the neck. It is quite likely that when break-up occurs close to one of the lobes, the most probable mass division would be one in which the near-spherical fragment carries away a few more nucleons than were originally present in the lobe. This would account for the fact that in all prompt mass distributions the maxima appear at about mass 135 and at some mass complementary to about mass 90. As the mass number of the fissioning nuclide increases, one would expect the hump in the 143-146 mass region (complement of mass 90) to move up in mass number, and this is also consistent with experimental observation. A schematic diagram illustrating the model is shown in Fig. V-6.

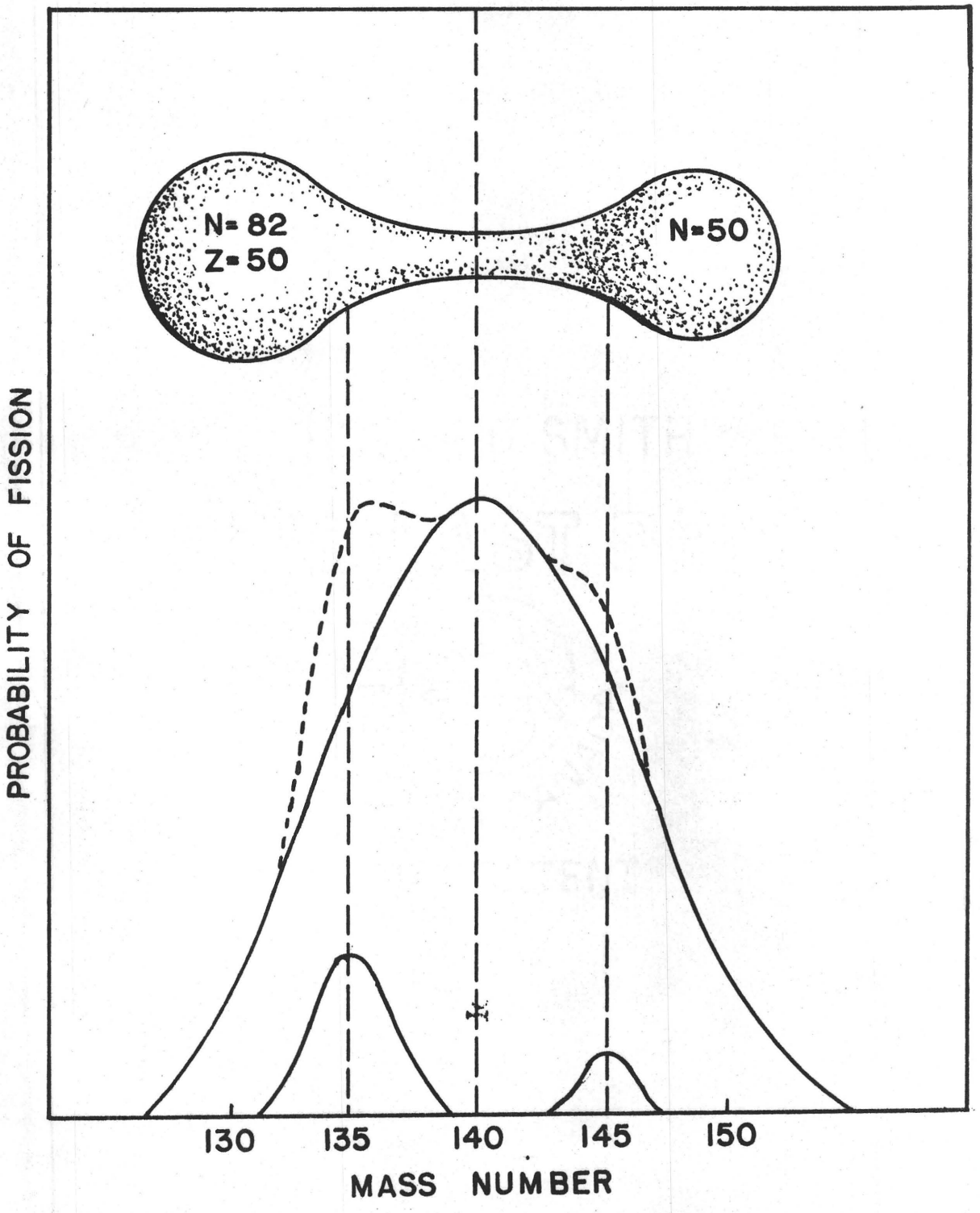

FIG. V-6: Speculative Picture of a Fissioning Nucleus

The observed mass distribution is taken to be the sum of the distributions corresponding to three different modes of fission.

In conclusion, it may be stated that, while most of the fine structure in the cumulative yield versus mass curve arises from the variation in neutron emission probabilities, some of it could be the effect of shell structure in the fission process.

GLOSSARY OF SYMBOLS

A	- Mass number of a nuclide
D_i	- Deformation energy
E	- Excitation energy of fission fragment
e	- Electronic charge
m	- Ratio of the masses of complementary fission fragments
$M^{*}c^2$	- Total energy of the compound nucleus (including excitation energy)
M_i	- Mass of the fission fragment i
N	- Neutron number
O	- Nuclear surface tension
$P_i(\cos \theta)$	- Legendre Polynomial
R	- Nuclear radius
$R_{(\theta)}$	- Nuclear radius as a function of angle
R_o	- $RA^{-1/3}$
s	- Distance between the centres of two fission fragments
T	- Total kinetic energy of fission fragments
V_k	- Nuclear potential between fragments
$W_o(E)$	- Nuclear level density at excitation energy E
x	- Fissionability parameter
Z	- Nuclear charge
α_i	- Coefficients in the expansion of $R_{(\theta)}$ in terms of Legendre Polynomials
β	- Deformation parameter of the nucleus as defined by Bohr and Mottelson (53B1)

γ - Ion-emission coefficient

ϕ - Neutron flux

ε - $(Z^2/A)_{\text{limiting}}$ in the liquid drop model

λ - Decay constant

$\mu = \frac{m_\pi c}{\hbar}$ where m_π is the mass of the π meson

ν - Reduced mass of the system consisting of two fission fragments in contact

σ - Nuclear surface tension
- Cross sections

BIBLIOGRAPHY

38N1 A. O. Nier, Phys. Rev. 53, 282.

38N2 A. O. Nier, Phys. Rev. 54, 275

39A1 H. L. Anderson, E. Fermi and H. B. Hanstein, Phys. Rev. 55, 797.

39B1 N. Bohr and J. A. Wheeler, Phys. Rev. 56, 426.

39F1 O. R. Frisch, Nature 143, 276.

39H1 O. Hahn and F. Strassmann, Naturwiss. 27, 11.

39H2 O. Hahn and F. Strassmann, Naturwiss. 27, 89.

39H3 O. Hahn and F. Strassmann, Naturwiss. 27, 529.

39J1 W. Jentschke and F. Prankl, Naturwiss. 27, 134.

39M1 L. Meitner and O. R. Frisch, Nature 143, 239, 471.

39vonH1 H. von Halban, Jr., F. Joliot and L. Kowarski, Nature 143, 470.

41A1 H. L. Anderson, E. Fermi and A. V. Grosse, Phys. Rev. 59, 52.

41M1 A. Moussa and L. Goldstein, Compt. rend. 212, 986.

46F1 J. Frenkel, J. Phys. (U.S.S.R.) 10, 533.

47A1 J. S. Allen, Rev. Sci. Instr. 18, 739.

47N1 A. O. Nier, Rev. Sci. Instr. 18, 398.

47Th1 H. G. Thode and R. L. Graham, Can. J. Res. A25, 1

48G1 W. E. Grummitt and G. Wilkinson, Nature 161, 520.

48I1 M. G. Inghram, D. C. Hess, Jr. and R. J. Hayden, Phys. Rev. 74, 98.

49G1 L. E. Glendenin, Mass Inst. Technol. Tech. Report No. 35.

50Br1 D. C. Brunton and G. C. Hanna, Can. J. Res. 28A, 190.

50Br2 D. C. Brunton and W. B. Thompson, Can. J. Res. 28A, 498.

50M1 T. Macnamara, C. B. Collins and H. G. Thode, Phys. Rev. 78, 129.

50W1 D. R. Wiles, Thesis, McMaster University, Hamilton, Ontario.

51C1 Radiochemical Studies: The Fission Products, edited by C. D. Coryell and N. Sugarman, National Nuclear Energy Series, Plutonium Project Record, Vol. 9, McGraw-Hill Publishing Co., New York.

51E1 D. W. Engelkemeir, J. A. Seiler, E. P. Steinberg and L. Winsberg, NNES IV-9, p. 1331.

51E2 D. W. Engelkemeir, M. S. Freedman, L. E. Glendenin and R. P. Metcalf, NNES IV-9, p. 1104.

51G1 L. E. Glendenin, E. P. Steinberg, M. G. Inghram and D. C. Hess, Phys. Rev. 84, 860.

51G2 L. E. Glendenin, C. D. Coryell and R. R. Edwards, NNES IV-9, p. 489.

52B1 I. Bergstrom, Arkiv Fysik 5, 191.

52L1 R. B. Leachman, Phys. Rev. 87, 444.

53B1 A. Bohr and B. R. Mottelson, K. Danske Vidensk. Selsk. Mat.-fys. Medd. 27, No. 16.

53F1 P. Fong, Phys. Rev. 89, 332.

53H1 D. L. Hill and J. A. Wheeler, Phys. Rev. 89, 1102.

53H2 D. J. Hughes, 'Pile Neutron Research', Addison-Wesley Publishing Co., Inc.

53In1 M. G. Inghram and W. A. Chupka, Rev. Sci. Instr. 24, (7), 518.

53P1 A. C. Pappas, Mass. Inst. Technol. Tech. Report No. 63.

53W1 D. R. Wiles, B. W. Smith, R. Horsley and H. G. Thode, Can. J. Phys. 31, 419.

54F1 J. S. Fraser and J. C. D. Milton, Phys. Rev. 93, 818.

54G1 A. E. S. Green, Phys. Rev. 95, 1006.

54K1 R. N. Keller, E. P. Steinberg and L. E. Glendenin, Phys. Rev. 94, 969.

54L1 R. B. Leachman and H. W. Schmitt, Phys. Rev. 96, 1366.

55P1 J. A. Petruska, H. G. Thode and R. H. Tomlinson, Can. J. Phys. 33, 693.

55P2 J. K. Perring and J. S. Storey, Phys. Rev. 98, 1525.

55W1 R. K. Wanless and H. G. Thode, Can. J. Phys. 33, 541.

55W2 D. M. Wiles and R. H. Tomlinson, Can. J. Phys. 33, 133.

56A1 K. Alder, A. Bohr, T. Huus, B. Mottelson and A. Winther, Rev. Mod. Phys. 28, 432.

56B1 A. Bohr, Paper No. P/911 in the Proceedings of the International Conference on the Peaceful Uses of Atomic Energy, United Nations, New York, 1956, Vol. 2.

56C1 R. L. Clarke, Symposium on the Physics of Fission, May 14-18, PM-322A, Atomic Energy of Canada Limited, Chalk River, Ontario.

56F1 P. Fong, Phys. Rev. 102, 434.

56I1 D. E. Irish, M.Sc. Thesis, McMaster University, Hamilton, Ontario.

56K1 T. J. Kennett, Ph.D. Thesis, McMaster University, Hamilton, Ontario.

56K2 G. R. Keepin, 'Progress in Nuclear Energy', Vol. I, Pergamon Press, London.

56S1 E. P. Steinberg and L. E. Glendenin, Paper No. P/614 in the Proceedings of the International Conference on the Peaceful Uses of Atomic Energy, United Nations, New York, 1956, Vol. 7.

56S2 R. P. Schuman, M. E. Jones and A. C. Mewherter, J. Inorg. Nucl. Chem. 3, 160.

57S1 W. E. Stein, Phys. Rev. 108, 94.

57S2 W. H. Sullivan, Trilinear Chart of Nuclides, U. S. Atomic Energy Commission.

58C1 J. G. Cuninghame, J. Inorg. Nucl. Chem. 5, 1.

58F1 H. R. Fickel and R. H. Tomlinson, Unpublished work, McMaster University, Hamilton, Ontario.

58Fd1 G. P. Ford, J. S. Gilmore, D. P. Ames, J. P. Balagna, J. W. Barnes, A. A. Comstock, et al, LA-1997.

58M1 J. C. D. Milton and J. S. Fraser, Phys. Rev. 111, 877.

58M2 B. P. Maksiutenko, J. Exp. Theore. Phys. (U.S.S.R.) 35, 815.

58Pr1 A. N. Protopopov, G. M. Tolmachev, V. N. Ushatskii, R. V. Venediktova, I. S. Krisiuk, L. P. Rodionova and G. N. Iakovleva, Atomnaya Energiya 5, 130.

58S1 W. E. Stein and S. L. Whetstone, Jr., Phys. Rev. 110, 476.

58W1 C. H. Westcott, A. E. C. L. No. 670, Chalk River, Ontario.

59B1 D. R. Bidinosti, H. R. Fickel and R. H. Tomlinson, Progress in Nuclear Energy, Series I, Vol. 3, p. 261.

59B2 D. R. Bidinosti, Ph.D. Thesis, McMaster University, Hamilton, Ontario.

59F1 H. R. Fickel and R. H. Tomlinson, Can. J. Phys. 37, 916.

59F2 H. R. Fickel, Ph.D. Thesis, McMaster University, Hamilton, Ontario.

59F3 H. R. Fickel and R. H. Tomlinson, Unpublished work, McMaster University, Hamilton, Ontario.

59H1 I. Halpern, Ann. Rev. Nucl. Sci. Vol. 9.

59W1 S. L. Whetstone, Jr., Phys. Rev. 114, 581.

60A1 V. K. Apalin, V. P. Dobrinin, V. P. Zaharova, I. E. Kutikov and L. A. Mikhaylan, Atomnaya Energiya 8, 15.

60B1 J. H. Beynon, 'Mass Spectrometry and its Application to Organic Chemistry', Elsevier Publishing Co.

60K1 S. Katcoff, Nucleonics 18, 201.

60T1 R. H. Tomlinson, private communication to S. Katcoff.

60W1 K. Way et al, Nuclear Data Sheets, 60-3-35, National Academy of Sciences, National Research Council, Washington 25, D. C.

61B1 W. Brunner and H. Paul, Annalen der Physik (7), 8, 146.

61B2 D. R. Bidinosti, D. E. Irish and R. H. Tomlinson, Can. J. Chem. 39, 628.

61B3 I. A. Baranov, A. N. Protopopov and V. P. Éismont, J. Exptl. Theoret. Phys. (U.S.S.R.) 41, 1003.

61F1 H. Farrar, A. K. Dasgupta and R. H. Tomlinson, Can. J. Chem. 39, 681.

62C1 W. B. Clarke, Ph.D. Thesis, McMaster University, Hamilton, Ontario.

62C2 S. Cohen and W. J. Swiatecki, Annals of Physics 19, 67.

62F1 H. Farrar and R. H. Tomlinson, Can. J. Phys. 40, 943.

62F2 H. Farrar, Ph.D. Thesis, McMaster University, Hamilton, Ontario.

62F3 H. Farrar and R. H. Tomlinson, Nuclear Physics 34, 367.

62H1 E. K. Hyde, 'A Revised Version of a Review of Nuclear Fission. Part One - Fission Phenomena at Low Energy', UCRL-9036Rev.

62H2 R. L. Henkel, unpublished data quoted in Ref. (62M2).

62K1 G. R. Keepin, Nucleonics 20,(8), 150.

62M1 J. C. D. Milton and J. S. Fraser, Can. J. Phys. 40, 1626.

62M2 J. H. Manley, Nuclear Physics 33, 70.

62T1 J. Terrel, Phys. Rev. 127, 880.

63F1 P. Fong, Phys. Rev. Letters 11, 375.

63F2 P. Fong, International Conference on Nuclear Physics with Reactor Neutrons, October 15-17, 1963, ANL-6797.

64T1 T. D. Thomas and R. Vandenbosch, Phys. Rev. 133, B976.

APPENDIX A: CONTRIBUTION OF PLUTONIUM FISSION TO THE SAMPLES OBTAINED BY IRRADIATING U^{238}

When U^{238} is irradiated in a nuclear reactor under cadmium wrap, it undergoes not only fission but also n,γ reaction. U^{238} nuclei capture neutrons to form U^{239}, which decays to Pu^{239} through Np^{239}. Even though both U^{239} and Np^{239} have fission cross sections too small to be of any significance, plutonium fission could contribute substantially to the fission products produced in long irradiations. The situation may be summarized as follows:

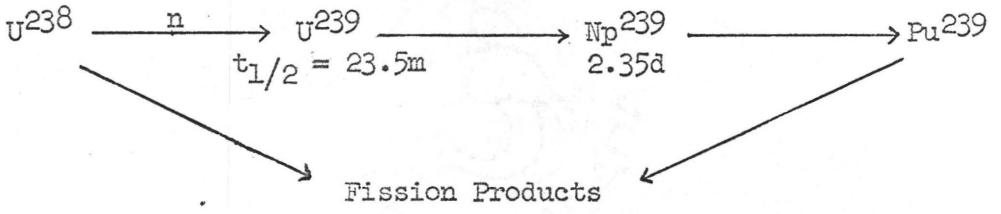

The half-life of U^{239} is very short as compared to the irradiation times and for all practical purposes Np^{239} may be considered as directly formed from U^{238}. Under these conditions the capture and decay chain may be represented as

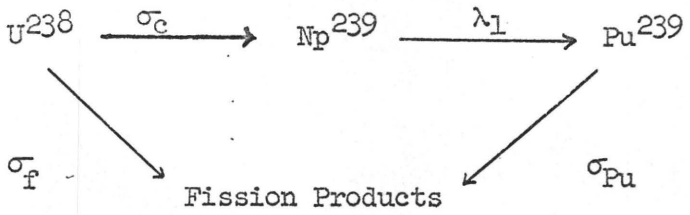

where the σ's and λ's are cross sections and decay constants respectively.

Let N be the original number of U^{238} nuclei present which changes regligibly during irradiation and N_1 and N_2 be the number of atoms of Np^{239} and Pu^{239}, respectively, present at time 't' during irradiation. If ϕ is the neutron flux, the rate of formation of Np^{239} is $N\sigma_c\phi$ and $N_1\lambda_1$ is its rate of decay. Then we have

$$\frac{dN_1}{dt} = N\sigma_c\phi - N_1\lambda_1$$

and hence $$N_1(t) = \frac{N\sigma_c\phi}{\lambda_1}\left[1 - e^{-\lambda_1 t}\right]$$

$$\frac{dN_2}{dt} = N_1(t)\lambda_1 - N_2\sigma_{Pu}\phi$$

Solving for N_2 we get

$$N_2 = N\sigma_c\phi\left[\frac{1 - e^{-\lambda_p t}}{\lambda_p} - \frac{e^{-\lambda_1 t} - e^{-\lambda_p t}}{\lambda_p - \lambda_1}\right]$$

where $\lambda_p = \sigma_{Pu}\phi$

The rate of plutonium fission at time t is $N_2(t)\lambda_p$. Therefore the total number of plutonium fissions formed in an irradiation for time T is given by

$$\int_0^T N_2(t)\,\lambda_p dt$$

$$= N\sigma_c\phi\lambda_p \int_0^T \left[\frac{1 - e^{-\lambda_p t}}{\lambda_p} - \frac{e^{-\lambda_1 t} - e^{-\lambda_p t}}{\lambda_p - \lambda_1}\right] dt$$

$$= N\sigma_c\phi T\left[1 + \frac{\lambda_1(1 - e^{-\lambda_p T})}{T\lambda_p(\lambda_p - \lambda_1)} - \frac{\lambda_p(1 - e^{-\lambda_1 T})}{T\lambda_1(\lambda_p - \lambda_1)}\right]$$

Since the number of U^{238} nuclei has changed very little, the total number of U^{238} fissions during an irradiation of time T is $N\sigma_f\phi_f T$.

Hence the ratio of plutonium fissions to uranium fissions is given by

$$\frac{\sigma_c \phi}{\sigma_f \phi_f}\left[1 + \frac{\lambda_1(1 - e^{-\lambda_1 T})}{T\,\lambda_p(\lambda_p - \lambda_1)} - \frac{\lambda_p(1 - e^{-\lambda_1 T})}{T\,\lambda_1(\lambda_p - \lambda_1)}\right]$$

Here $(\sigma_f \phi_f)$ is the rate of fission per atom of U^{238} and $\sigma_{Pu}\phi$ is the rate of fission per atom of Pu^{239} under the conditions of irradiation.

The ratio $\sigma_c\phi/\sigma_f\phi_f$ was directly measured by irradiating U^{238} for a short time in the reactor under cadmium wrap and comparing the Np^{239} and Ba^{139} produced. The latter isotopes were separated using the usual radiochemical techniques and the γ-spectra were compared. The observed value for $\sigma_c\phi/\sigma_f\phi_f$ was about 62.5.

$\sigma_{Pu}\phi$ was estimated using the known value of cadmium ratio for Co^{59} under the same irradiation conditions. We know that

$$\sigma_{Pu}\phi = \phi_{ep} \int_{0.4\ ev}^{\infty} \sigma_{Pu}(E)\ \frac{dE}{E} \qquad (53H2)$$

where ϕ_{ep} is the resonance flux in a logarithmic energy interval and E is energy.

$\int_{E = 0.4\ ev}^{E = \infty} \sigma_{Pu}(E)\ \frac{dE}{E}$, the resonance integral for Pu^{239} is known to be 250 b.

For any nuclide,

$$\int_{0.4\ ev}^{\infty} \sigma(E)\ \frac{dE}{E} = \frac{\sigma_{th}}{R_{Cd} - 1}\ \frac{\phi_{th}}{\phi_{ep}} \qquad (53H2)$$

where σ_{th} is its thermal neutron cross section,

ϕ_{th} is the thermal flux and

R_{Cd} is the cadmium ratio

For Co^{59} we know that σ_{th} is 36.6 barns and the resonance integral is 48 barns (58W1). The cadmium ratio under the conditions of irradiation used in this work was about 15.

Hence $$\frac{\phi_{th}}{\phi_{ep}} \approx 18.5$$

Knowing ϕ_{th} (1.5×10^{13} neutrons/cm^2/sec), we can calculate ϕ_{ep} and hence $\sigma_{Pu}\phi$. Using these values one finds that the number of Pu^{239} fission is under 3% of the number of U^{238} fission for a 54-day irradiation.

APPENDIX B: DECAY CORRECTIONS INVOLVED IN CONVERTING A MEASURED ABUNDANCE RATIO TO RELATIVE CHAIN YIELD

The fission yield of a given mass number is distributed along an isobaric chain. At the time of abundance measurement, most of the chain is decayed to one or more of the end members. Decay correction involves the conversion of the measured ratio, which represents the number of atoms of a particular nuclide of the chain at the time of measurement, to the relative chain yield which represents the total number of atoms belonging to the chain formed in fission.

The decay correction may be illustrated by means of a specific example. Consider the mass 133 chain.

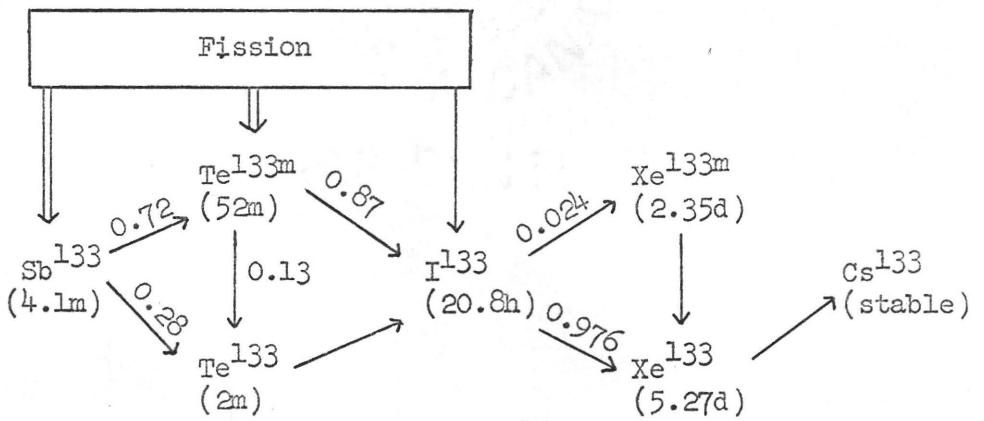

The early members of the chain are short-lived and xenon and cesium are formed in such low independent yields that, from the point of view of the present discussion, the entire chain may be thought of as being formed in fission as I^{133}, which then decays down the chain. Because of the branching we can split the decay into two chains.

I. Consider the chain

$$I^{133} \underset{(N_1)}{\xrightarrow[(0.976)]{\lambda_1}} Xe^{133} \underset{(N_{2g})}{\xrightarrow{\lambda_3}} Cs^{133} \underset{(N_3)}{}$$

The N's represent the number of nuclei of each species present at some time during irradiation.

If R is the rate of fission, we have

$$\frac{dN_1}{dt} = R - N_1\lambda_1$$

$$\frac{dN_{2g}}{dt} = 0.976\, N_1\lambda_1 - N_{2g}\lambda_3$$

Solving these differential equations and setting the time as T (representing the end of irradiation), we get

$$N_{2g} = 0.976\, R \left[\frac{1 - e^{-\lambda_3 T}}{\lambda_3} - \frac{e^{-\lambda_1 T} - e^{-\lambda_3 T}}{\lambda_3 - \lambda_1}\right]$$

After a cooling period 't', this becomes

$$N'_{2g}(t) = 0.976\, R \left[\frac{1 - e^{-\lambda_3 T}}{\lambda_3} - \frac{e^{-\lambda_1 T} - e^{-\lambda_3 T}}{\lambda_3 - \lambda_1}\right] e^{-\lambda_3 t}$$

But some $Xe^{133}_{(N''_{2g})}$ is also produced during cooling from the decay of I^{133}.

$$\frac{dN''_{2g}(t)}{dt} = 0.976\, N_1\lambda_1 - N''_{2g}(t)\lambda_3 \qquad \text{(during cooling)}$$

$$\text{Hence } N''_{2g}(t) = 0.976R\,(1 - e^{-\lambda_1 T}) \left[\frac{e^{-\lambda_1 t} - e^{-\lambda_3 t}}{\lambda_3 - \lambda_1}\right]$$

The total number of Xe^{133} atoms, then, at time t is

$$N_{2g}(t) = N'_{2g}(t) + N''_{2g}(t) =$$

$$= 0.976\,R \left[\frac{(1 - e^{-\lambda_1 T})e^{-\lambda_1 t}}{\lambda_3 - \lambda_1} - \frac{\lambda_1(1 - e^{-\lambda_3 T})e^{-\lambda_3 t}}{\lambda_3(\lambda_3 - \lambda_1)}\right]$$

II. Consider the chain

$$\underset{(N_1)}{I^{133}} \xrightarrow[0.024]{\lambda_1} \underset{(N_{2m})}{Xe^{133m}} \xrightarrow{\lambda_2} \underset{(N_{2g})}{Xe^{133}} \xrightarrow{\lambda_3} \underset{(N_3)}{Cs^{133}}$$

The number of Xe^{133m} atoms present at the end of irradiation and decay is

$$N_{2m}(t) = 0.024\,R \left[\frac{(1 - e^{-\lambda_1 T})e^{-\lambda_1 t}}{\lambda_2 - \lambda_1} - \frac{\lambda_1(1 - e^{-\lambda_2 T})e^{-\lambda_2 t}}{\lambda_2(\lambda_2 - \lambda_1)}\right]$$

In addition, some Xe^{133} is formed through the decay of Xe^{133m}, both during irradiation ($N_{2g'}$ atoms) and cooling ($N_{2g''}$ atoms).

$$\frac{dN_{2g'}}{dt} = N_{2m}\lambda_2 - N_{2g'}\lambda_3 \quad \text{(net rate of formation of } Xe^{133} \text{ during irradiation)}$$

$$\frac{dN_{2g''}}{dt} = N_{2m}\lambda_2 - N_{2g''}\lambda_3 \quad \text{(net rate of formation of } Xe^{133} \text{ during cooling)}$$

Solving these equations we get the total number of Xe^{133} atoms formed through the decay of Xe^{133m} as

$$N^{m}_{2g}(t) = N_{2g'} + N_{2g''}$$

$$= 0.024\, R\lambda_2 \left[\left\{ \frac{(1 - e^{-\lambda_1 T})e^{-\lambda_1 t}}{(\lambda_2 - \lambda_1)(\lambda_3 - \lambda_1)} - \frac{\lambda_1 (1 - e^{-\lambda_2 T})e^{-\lambda_2 t}}{\lambda_2(\lambda_2 - \lambda_1)(\lambda_3 - \lambda_2)} \right\} \right.$$

$$\left. + \left\{ \frac{1}{\lambda_2 \lambda_3} - \frac{1}{(\lambda_2 - \lambda_1)(\lambda_3 - \lambda_1)} + \frac{\lambda_1}{\lambda_2(\lambda_2 - \lambda_1)(\lambda_3 - \lambda_2)} \right\} (1 - e^{-\lambda_3 T})e^{-\lambda_3 t} \right]$$

Thus the total $N_{2g}(t)$ is

$$0.976\, R \left[\frac{(1 - e^{-\lambda_1 T})e^{-\lambda_1 t}}{\lambda_3 - \lambda_1} - \frac{\lambda_1 (1 - e^{-\lambda_3 T})e^{-\lambda_3 t}}{\lambda_3(\lambda_3 - \lambda_1)} \right]$$

$$+ 0.024\, R\lambda_2 \left[\left\{ \frac{(1 - e^{-\lambda_1 T})e^{-\lambda_1 t}}{(\lambda_2 - \lambda_1)(\lambda_3 - \lambda_1)} - \frac{\lambda_1 (1 - e^{-\lambda_2 T})e^{-\lambda_2 t}}{\lambda_2(\lambda_2 - \lambda_1)(\lambda_3 - \lambda_2)} \right\} \right.$$

$$\left. + \left\{ \frac{1}{\lambda_2 \lambda_3} - \frac{1}{(\lambda_2 - \lambda_1)(\lambda_3 - \lambda_1)} + \frac{\lambda_1}{\lambda_2(\lambda_2 - \lambda_1)(\lambda_3 - \lambda_2)} \right\} (1 - e^{-\lambda_3 T})e^{-\lambda_3 t} \right]$$

and the total N_{2m} is

$$0.024\, R \left[\frac{(1 - e^{-\lambda_1 T})e^{-\lambda_1 t}}{\lambda_2 - \lambda_1} - \frac{\lambda_1 (1 - e^{-\lambda_2 T})e^{-\lambda_2 t}}{\lambda_2(\lambda_2 - \lambda_1)} \right]$$

If t_1 is the time between extraction and measurement, then the total number of Xe^{133} and Xe^{133m} atoms at time t_1 is given by

$$N^{133}_{(t_1)} = N_{2g}\, e^{-\lambda_3 t_1} + N_{2m}\left[e^{-\lambda_2 t_1} + \frac{\lambda_2}{\lambda_3 - \lambda_2}\left(e^{-\lambda_2 t_1} - e^{-\lambda_3 t_1}\right)\right]$$

The total number of mass 133 atoms formed (during irradiation) is RT. Hence the correction factor is

$$f = \frac{RT}{N^{133}(t_1)}$$

Evidently the correction factor for Cs^{133} is

$$\frac{f}{f - 1}.$$